THE JOURNAL OF BIOLOGICAL CHEMISTRY VOL. 283, NO. 39, pp. 26643–26661, September 26, 2008

Acute Hypertonicity Alters Aquaporin-2 Trafficking and Induces a MAPK-dependent Accumulation at the Plasma Membrane of Renal Epithelial Cells*

Received for publication, February 8, 2008, and in revised form, June 10, 2008 Published, JBC Papers in Press, July 29, 2008, DOI 10.1074/jbc.M801071200

Udo Hasler[1], Paula Nunes[2], Richard Bouley[3], Hua A. J. Lu[4], Toshiyuki Matsuzaki, and Dennis Brown

From the Massachusetts General Hospital Center for Systems Biology, Program in Membrane Biology and Nephrology Division, Massachusetts General Hospital and Department of Medicine, Harvard Medical School, Boston, Massachusetts 02114-2790

The unique phenotype of renal medullary cells allows them to survive and functionally adapt to changes of interstitial osmolality/tonicity. We investigated the effects of acute hypertonic challenge on AQP2 (aquaporin-2) water channel trafficking. In the absence of vasopressin, hypertonicity alone induced rapid (<10 min) plasma membrane accumulation of AQP2 in rat kidney collecting duct principal cells *in situ*, and in several kidney epithelial lines. Confocal microscopy revealed that AQP2 also accumulated in the *trans*-Golgi network (TGN) following hypertonic challenge. AQP2 mutants that mimic the Ser^{256}-phosphorylated and -nonphosphorylated state accumulated at the cell surface and TGN, respectively. Hypertonicity did not induce a change in cytosolic cAMP concentration, but inhibition of either calmodulin or cAMP-dependent protein kinase A activity blunted the hypertonicity-induced increase of AQP2 cell surface expression. Hypertonicity increased p38, ERK1/2, and JNK MAPK activity. Inhibiting MAPK activity abolished hypertonicity-induced accumulation of AQP2 at the cell surface but did not affect either vasopressin-dependent AQP2 trafficking or hypertonicity-induced AQP2 accumulation in the TGN. Finally, increased AQP2 cell surface expression induced by hypertonicity largely resulted from a reduction in endocytosis but not from an increase in exocytosis. These data indicate that acute hypertonicity profoundly alters AQP2 trafficking and that hypertonicity-induced AQP2 accumulation at the cell surface depends on MAP kinase activity. This may have important implications on adaptational processes governing transcellular water flux and/or cell survival under extreme conditions of hypertonicity.

Most mammalian cells are exposed to an extracellular environment that remains isotonic under normal physiological conditions, largely as a result of renal regulatory mechanisms that maintain water and electrolyte body fluid composition within a very narrow range. This process relies on the countercurrent concentration mechanism that occurs along the loop of Henle and which, in turn, depends on the generation of a NaCl and urea concentration gradient along the cortico-papillary axis. As a consequence, renal medullary cells are physiologically exposed to changing conditions of variable interstitial osmolality/tonicity that can reach up to 1200 mosmol/kg in human inner medulla and up to 4500 mosmol/kg in some remarkable rodent species that are adapted to life in arid desert conditions (1). The unique phenotype of these cells allows them to survive and function under these "hostile" conditions and to rapidly adapt to recurrent variations in their environmental tonicity that follow physiological and behavioral changes. In addition to the promotion of intracellular events that ensure cell survival, hypertonicity also promotes events that mediate changes in cell function in various physiological settings. Both rapid and slow responses mediate cell adaptation to increased extracellular tonicity. Rapid responses include actin and microtubule remodeling, changes in phosphoinositide metabolism, and activation of a large network of intracellular signaling pathways, including MAPK[5] and tyrosine kinase pathways (2–5). The slower transcriptional response triggered by hypertonicity mediates numerous long term events, such as those involved in reducing cellular ionic strength and reinstating cell growth (6, 7).

The final adjustment of the water reabsorption process occurs at the level of the collecting duct (CD) and is largely under the control of the antidiuretic hormone vasopressin (VP). An acute increase of plasma VP concentration leads to an accumulation of the AQP2 (aquaporin-2) water channel at the

* This work was supported, in whole or in part, by National Institutes of Health Grant DK38452 (to D. B.). The Microscopy Core facility of the Massachusetts General Hospital Program in Membrane Biology receives additional support from the Boston Area Diabetes and Endocrinology Research Center (DK57521) and the Center for the Study of Inflammatory Bowel Disease (DK43341). The costs of publication of this article were defrayed in part by the payment of page charges. This article must therefore be hereby marked "*advertisement*" in accordance with 18 U.S.C. Section 1734 solely to indicate this fact.

[1] Supported by a Swiss Fondation Suisse pour les Bourses en Médecine et Biologie Fellowship and an Executive Committee on Research Fellowship from Massachusetts General Hospital. To whom correspondence should be addressed: Service de Néphrologie, Fondation pour Recherches Médicales, 64 Avenue de la Roseraie, CH-1211, Geneva 4, Switzerland. Tel.: 617-726-7496; Fax: 617-643-3182; E-mail: Udo.Hasler@medecine.unige.ch.

[2] Supported by a doctoral level postgraduate scholarship from Natural Sciences and Engineering Council of Canada.

[3] Recipient of a Young Investigator Award from the National Kidney Foundation.

[4] Supported by National Institutes of Health KO8 Grant DK075940-01.

[5] The abbreviations used are: MAPK, mitogen-activated protein kinase; CD, collecting duct; VP, vasopressin; V_2R, vasopressin receptor type 2; PKA, cAMP-dependent protein kinase A; ERK, extracellular signal-regulated kinase; JNK, c-Jun N-terminal kinase; YFP, yellow fluorescent protein; ssYFP, soluble secreted yellow fluorescent protein; GFP, green fluorescent protein; MDCK, Madin-Darby canine kidney; PBS, phosphate-buffered saline; BisTris, 2-[bis(2-hydroxyethyl)amino]-2-(hydroxymethyl)propane-1,3-diol; IBMX, 3-isobutyl-1-methylxanthine; FITC, fluorescein isothiocyanate; IOD, integrated optical density; TGN, *trans*-Golgi network; MEK, mitogen-activated protein kinase/extracellular signal-regulated kinase kinase; mβCD, methyl-β-cyclodextrin; SNAP, soluble *N*-ethylmaleimide-sensitive factor attachment protein; SNARE, SNAP receptor; PKI, PKA inhibitor; MDC, monodansylcadaverine.

apical surface of CD principal cells, providing a means by which luminal water can enter the cell (8). Driven by the osmotic gradient, water exits the cell via AQP3 and AQP4 expressed in the basolateral membrane. The effect of VP on AQP2 trafficking is mediated by vasopressin receptor type 2 (V_2R) mainly located in the basolateral membrane of CD principal cells. V_2R activation by VP leads to activation of the $G_s\alpha$/adenylyl cyclase system, increased cAMP concentration, and cAMP-dependent protein kinase A (PKA) activation (9). Phosphorylation of AQP2 at Ser^{256} is essential for AQP2 accumulation at the cell surface (10). In addition to VP, other factors modulate AQP2 expression at the cell surface. These include dopamine, prostaglandin E_2, and agents that increase cGMP concentration (11–13).

Osmotic challenge to cells in the kidney is greatest in the inner medulla and gradually decreases through the outer medulla and toward the cortex. Several pieces of experimental evidence have shown that, together with VP, hypertonicity plays a major role in enhancing AQP2 gene transcriptional activity (14–19). Chronic hypertonicity was additionally shown to facilitate VP-induced AQP2 insertion into the basolateral membrane of CD principal cells (20). Renal medullary cells are routinely exposed to abrupt variations of extracellular tonicity that challenge cell volume homeostasis. Induction of AQP2 internalization from the surface of renal CD8 cells was recently shown to occur immediately following *hypotonic* challenge (21), possibly reflecting a role that AQP2 may play in regulatory volume decrease mechanisms. In light of the key role that AQP2 plays in mediating luminal water entry into CD principal cells, we investigated whether altered AQP2 trafficking and plasma membrane expression occur as a rapid response to *hypertonic* challenge. To this end, we analyzed AQP2 expression following acute hypertonic challenge in kidney tissue slices and in both $mCCD_{cl1}$ cells, a recently established and spontaneously transformed mouse cell line derived from cortical collecting duct primary cultures (22), and well characterized LLC-PK_1 cells that stably express c-*myc*-tagged AQP2 (23–26). We show that, remarkably, acute (≤30 min) hypertonic challenge increases AQP2 expression at the plasma membrane in all three models to levels comparable with that achieved by VP alone. This occurs independently of a rise in cAMP content, depends on Ser^{256} phosphorylation, and is at least partly mediated by p38, extracellular signal-regulated kinase (ERK), and c-Jun N-terminal kinase (JNK) signaling pathways.

EXPERIMENTAL PROCEDURES

AQP2 Constructs and Cell Culture—LLC-PK_1 cells expressing wild-type AQP2 were named LLC-AQP2 (24). The production of stably transfected LLC-PK_1 cells expressing an AQP2 S256A mutant that mimics nonphosphorylated AQP2 (LLC-AQP2 (S256A)) was previously described (10). Following the same procedure, LLC-PK_1 cells were stably transfected with c-*myc*-tagged AQP2 inserted in the pcDNA1/Neo vector in which Ser^{256} was replaced with aspartate (LLC-AQP2 (S256D)) in order to mimic phosphorylated AQP2. LLC-AQP2 cells expressing soluble secreted yellow fluorescent protein (ssYFP; see below) are referred to as LLC-ssYFP. LLC-AQP2 cells expressing GFP-tagged V_2R (27) are referred to as LLC-V_2R-GFP. For the creation of stably transfected MDCK cells that express c-*myc*-tagged wild-type AQP2 (MDCK-AQP2), cDNA encoding AQP2 epitope-tagged with a 30-bp tail encoding a 10-amino acid c-*myc* peptide was transfected into MDCK cells as previously described for LLC-PK_1 cells (24). $mCCD_{cl1}$ cells, which express endogenous AQP2,[6] were seeded on permeable filters (Transwell®; Corning Glass) and grown in culture medium supplemented with 2% fetal calf serum (22). All other cells were seeded on glass coverslips and grown in Dulbecco's modified Eagle's medium (Invitrogen) supplemented with 10% (v/v) fetal calf serum. Confluent cells were grown in serum- and hormone-free medium for 1 h (for LLC-PK_1 and MDCK cells) or 24 h (for $mCCD_{cl1}$ cells) before performing experiments. Isoosmotic (300 mosmol/kg) medium was made hypertonic by replacing a fraction of the medium with NaCl-enriched medium (1100 mosmol/kg) to obtain 350–600 mosmol/kg medium. For control cells, the same fraction of medium was replaced by isotonic medium. Medium osmolality was checked using an osmometer. For VP stimulation, 10 nM [Lys^8] vasopressin was used for LLC-AQP2 cells and 10 nM [Arg^8] vasopressin was used for $mCCD_{cl1}$ cells.

Preparation of Rat Kidney Slices—Adult vasopressin-deficient Brattleboro rats were purchased from Harlan Sprague-Dawley (Indianapolis, IN). Animals were thirsted for 12 h, as previously described (28), and anesthetized with an intraperitoneal injection of sodium pentobarbital (65 mg/kg). Both kidneys were removed, cut into 2–3-mm-thick slices using a razor blade, and quickly placed in Hanks' balanced salt solution (110 mM NaCl, 5 mM KCl, 1.2 mM $MgSO_4$, 1.8 mM $CaCl_2$, 4 mM sodium acetate, 1 mM Na_3 citrate, 6 mM D-glucose, 6 mM L-alanine, 1 mM NaH_2PO_4, 3 mM Na_2HPO_4, 25 mM $NaHCO_3$, pH 7.4) at 37 °C equilibrated with 5% CO_2, 95% O_2. Slices 0.5 mm in thickness were then cut with a Stadie-Riggs microtome (Thomas Scientific, Swedesboro, NJ) as previously described (29). The slices were first incubated at 37 °C for 15 min in equilibrated Hanks' balanced solution to establish base-line resting conditions and then stimulated for various periods of time with 100 nM [Arg^8]vasopressin or with NaCl-enriched hypertonic medium. The slices were fixed in 4% paraformaldehyde containing 10 mM sodium periodate and 75 mM lysine, as previously described (29). Slices were then rinsed several times with phosphate-buffered saline (PBS), and 4-μm-thick cryosections were prepared as previously described (23). After rehydration in PBS for 15 min, sections were treated with 1% SDS prior to blocking and immunostaining of sections described below.

Immunocytochemistry—Control and stimulated cultured cells were immediately fixed in PBS, pH 7.4, containing 4% (w/v) paraformaldehyde and 5% (w/v) sucrose for 20 min, washed in PBS, permeabilized with Triton X-100 (0.1%, v/v) for 3–5 min, and then washed in PBS. Nonspecific antibody binding to permeabilized cultured cells and kidney slices was blocked with 1% (w/v) bovine serum albumin in PBS for 30 min prior to a 1-h incubation with primary monoclonal mouse anti-

[6] U. Hasler, P. Nunes, R. Bouley, H. A. J. Lu, T. Matsuzaki, and D. Brown, unpublished data.

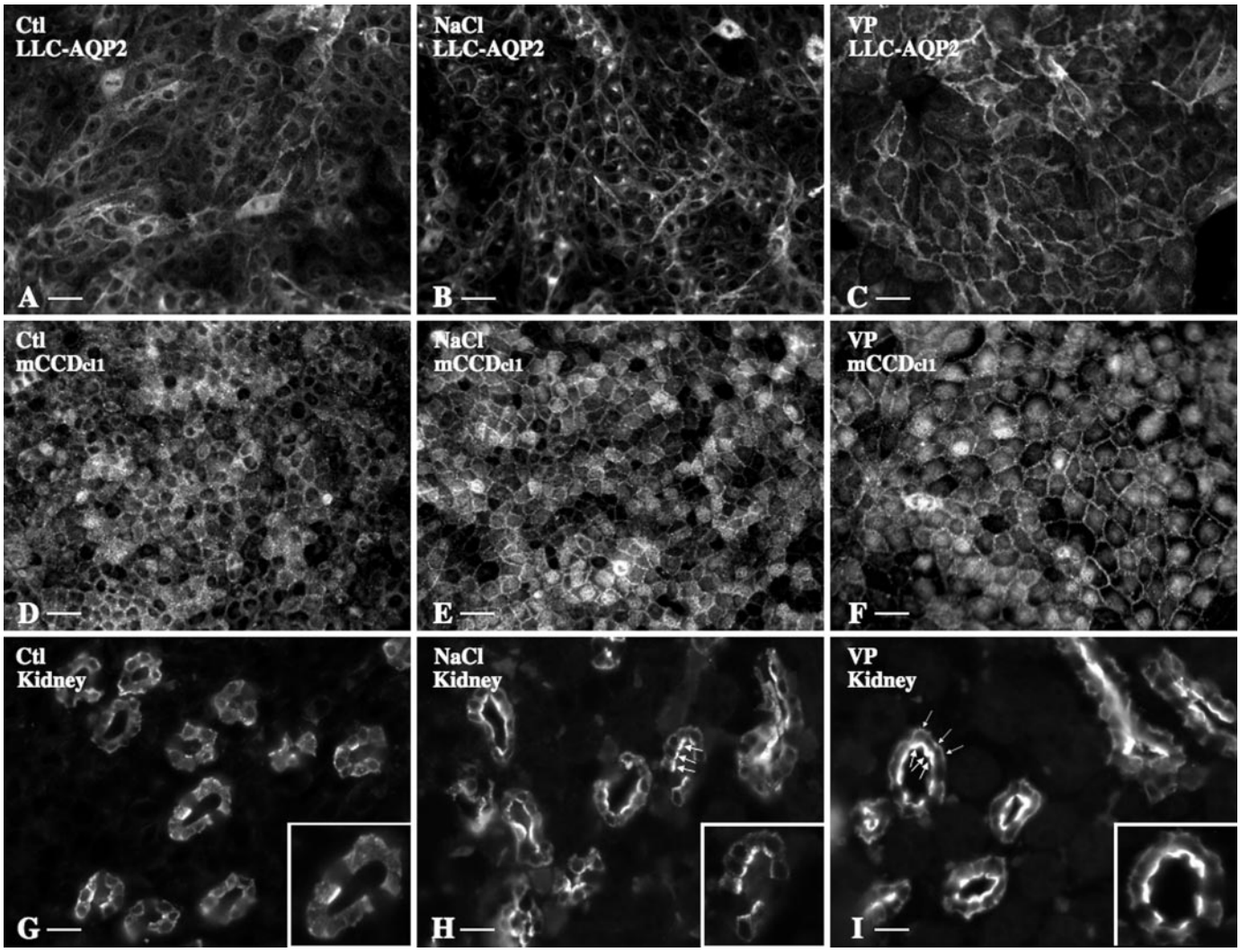

FIGURE 1. **Acute hypertonicity increases AQP2 expression at the cell surface.** LLC-AQP2 cells (*A–C*), mCCDcl$_1$ cells (*D–F*), and rat kidney slices (*G–I*) were challenged or not (*Ctl*) for 30 min with either NaCl-enriched hypertonic (500 mosmol/kg) medium or VP prior to fixation and staining with anti-c-*myc* (for LLC-AQP2 cells) or anti-AQP2 (for mCCDcl$_1$ cells and kidney slices) antibodies. *G–I*, AQP2 immunostaining in the proximal inner medulla. *Large arrowheads*, AQP2 expressed at the apical membrane; *small arrowheads*, indicate AQP2 expressed at the basal membrane. *Bar*, 10 μm (*A–F*) and 5 μm (*G–I*).

body against c-*myc* (30), primary polyclonal rabbit antibody against a stretch of amino acids corresponding to Glu^{250}–Gln^{263} of the AQP2 c-terminus, primary monoclonal mouse antibody against clathrin heavy chain (2.5 μg/ml; Transduction Laboratories, Palo Alto, CA), primary monoclonal mouse antibody against Golgin-97 (1:200 dilution; Invitrogen), or primary polyclonal goat antibody against Glut1 (4 μg/ml; Santa Cruz Biotechnology, Inc., Santa Cruz, CA). Cells were then washed with PBS and incubated for 1 h with donkey anti-mouse antibody conjugated to indocarbocyanine (0.4 μg/ml; Jackson ImmunoResearch, West Grove, PA), donkey anti-rabbit antibody conjugated to fluorescein (5 μg/ml; Jackson ImmunoResearch), goat anti-mouse antibody conjugated to Alexa Fluor 488 (40 μg/ml; Invitrogen), or donkey anti-goat antibody conjugated to indocarbocyanine (2 μg/ml; Jackson ImmunoResearch). For double staining experiments, Glut1, clathrin, and golgin-97 staining was performed prior to AQP2 staining. Specimens were mounted in Vectashield (Vector Laboratories, Burlingame, CA) and examined using a Nikon Eclipse 80i epifluorescence microscope coupled to a Hamamatsu Orca CCD camera or using a Zeiss Radiance 2000 confocal laser-scanning microscope (Carl Zeiss, Oberkochen, Germany). Images were taken with a Plan Apo ×40/1.0 numerical aperture Nikon objective (for epifluorescent microscopy) or a Plan Apo ×63/1.4 numerical aperture Zeiss objective (for confocal microscopy) and acquired using IPLab software (BD Biosciences Bioimaging, Rockville, MD). For *x-z* scan analysis of AQP2 expression at the cell surface, confluent LLC-AQP2 cells were treated with 2.5 μg/ml wheat germ agglutinin conjugated with Alexa Fluor 488 (Invitrogen) for 5 min prior to cell fixation and AQP2 staining. *x-z* planes of confocal microscope images taken at 0.15-μm intervals were reconstructed by Volocity software (Improvision, Lexington, MA).

Biotinylation—Expression levels of AQP2 at the apical surface of LLC-AQP2 cells were semiquantified by growing cells to confluence on permeable 12-mm diameter filters (Costar) and treating cells or not (control) with either VP (10 nM) or hypertonic medium (500 mosmol/kg) for 30 min. Cells were then placed on ice, and the basal medium was immediately replaced with ice-cold PBS while the apical medium was

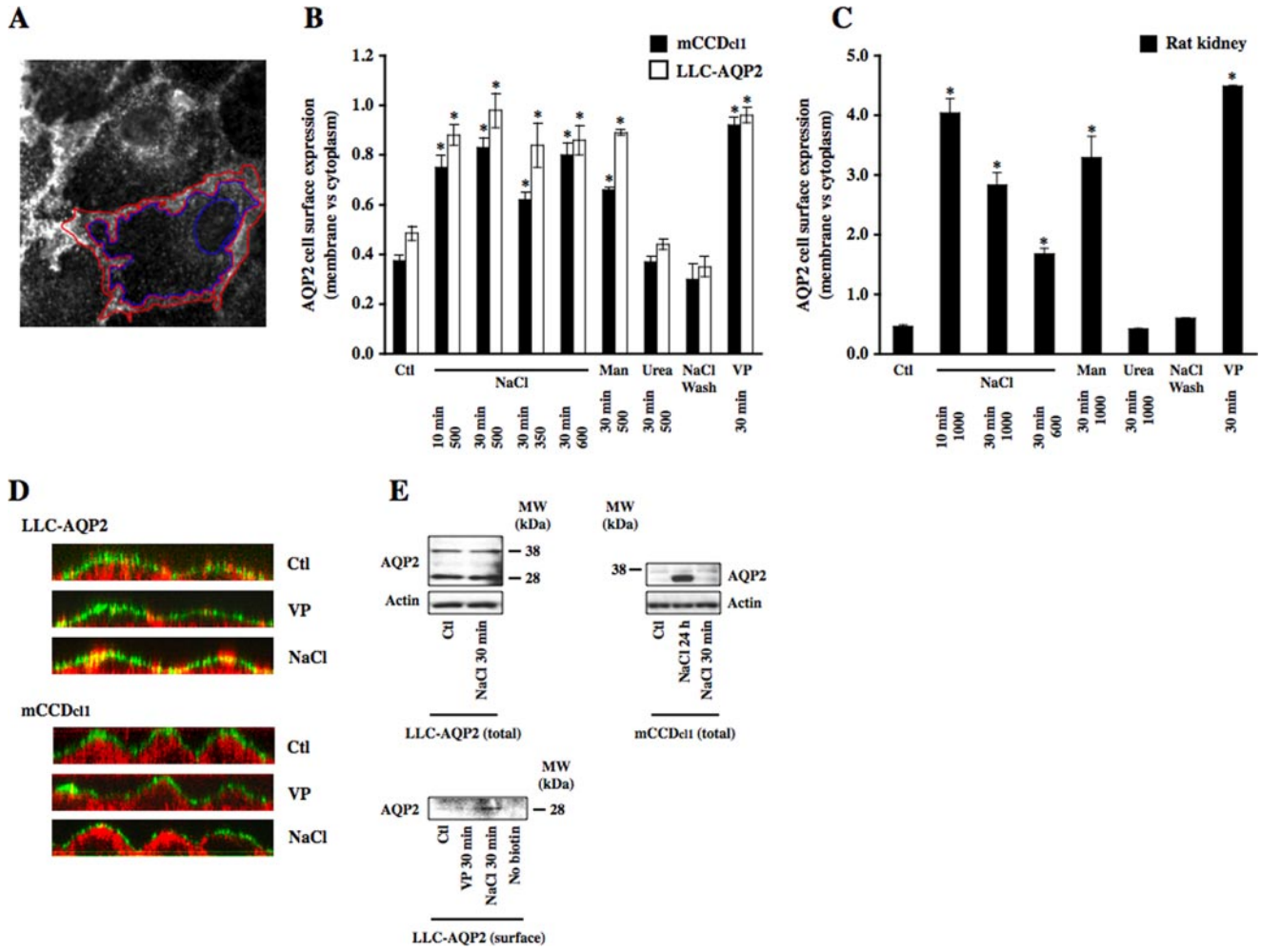

FIGURE 2. **A small increase of extracellular tonicity induces a rapid and reversible accumulation of AQP2 at the cell surface.** *A*, AQP2 expression at the cell surface and cytoplasm was estimated using IPLab software by quantifying the number of pixels contained in an outline enclosing the plasma membrane (highlighted in *red*) and the cell cytoplasm (highlighted in *blue*). A representative image of a VP-challenged LLC-AQP2 cell is shown. *B* and *C*, mCCDcl$_1$ cells (*B*, *closed bars*), LLC-AQP2 cells (*B*, *open bars*), and rat kidney slices (*C*) were challenged or not (*Ctl*) for 10 or 30 min with NaCl-enriched hypertonic (350–1000 mosmol/kg) medium, mannitol (*Man*)-enriched hypertonic (500 or 1000 mosmol/kg) medium, urea-enriched hyperosmotic (500 or 1000 mosmol/kg) medium, or VP. In another set of experiments, cells and kidney slices were first challenged with NaCl-enriched hypertonic (500 and 1000 mosmol/kg for cell lines and for kidney slices, respectively) medium for 30 min, after which time the medium was replaced by isotonic medium followed by an additional 30 min of incubation (NaCl wash). Cells were fixed and stained as described for Fig. 1, and AQP2 cell surface expression was determined as described in *A* and under "Experimental Procedures." Results are mean ± S.E. ($n = 3$–5). *, $p < 0.05$. *D*, *x-z* scan analysis of confocal images of LLC-AQP2 and mCCD$_{cl1}$ cells challenged or not (*Ctl*) for 30 min with VP or NaCl-enriched hypertonic (500 mosmol/kg) medium. Hypertonicity induced AQP2 (*red*) to rapidly redistribute toward apical and lateral poles of both cell lines. The plasma membrane was visualized by Alexa Fluor 488-conjugated wheat germ agglutinin (*green*). AQP2 expression at the cell surface is revealed in *yellow*. Representative images of four independent experiments are shown. *E*, Western blot analysis of total protein extracts of LLC-AQP2 and mCCD$_{cl1}$ cells (*top*) and streptavidin-agarose-precipitated biotinylated AQP2 expressed at the apical surface of LLC-AQP2 cells (*bottom*). Although 30 min of hypertonic challenge increased AQP2 expression at the apical surface of LLC-AQP2 cells, it did not affect whole-cell AQP2 abundance. Apical AQP2 was not detected in cells that were not labeled with biotin (*No biotin*). Whole-cell AQP2 abundance in mCCD$_{cl1}$ cells was not altered by 30 min of hypertonic challenge but increased 12-fold after 24 h of hypertonic stimulation, similar to the effect previously observed in mpkCCD$_{cl4}$ cells (15). Actin was used as a loading control for whole-cell lysates. Representative images of three independent experiments are shown.

replaced with PBS or 5 mg/ml EZ-Link sulfosuccinimidyl-6-(biotinamido)hexanoate (Thermo Scientific, Waltham, MA) in PBS. After 1 h of incubation at 4 °C, cells were rinsed twice with ice-cold PBS-CM (PBS containing 1 mM $MgCl_2$ and 0.1 mM $CaCl_2$). Free biotin was then quenched with a 10-min incubation of 50 mM NH_4Cl in PBS at 4 °C. Cells were washed twice with PBS-CM at 4 °C cells, scraped off of filters (3 filters/condition), and spun down. Cells were then resuspended in 250 μl of lysis buffer (20 mM Tris-HCl, pH 8.0, 150 mM NaCl, 5 mM EDTA, 1% Triton X-100, 0.2% bovine serum albumin, 1 mM phenylmethylsulfonyl fluoride, 5 μg/ml leupeptin and pepstatin), sonicated four times for 20 s each, incubated for 20 min at 37 °C, and spun at 14,000 × *g* for 1 min. The supernatant was then incubated 24 h at 4 °C with streptavidin-agarose beads (Thermo Scientific) that were preincubated overnight at 4 °C with lysis buffer and added to the supernatant at a 1:5 ratio. The beads were washed three times with ice-cold lysis buffer and then twice with lysis buffer without bovine serum albumin prior to the addition of loading buffer. Samples were then heated at 65 °C for 10 min, and the supernatant was analyzed by SDS-PAGE using a monoclonal mouse antibody against c-*myc* (30).

Western Blot Analysis—Preparation of total cell lysate was performed as previously described (15). Equal amounts of pro-

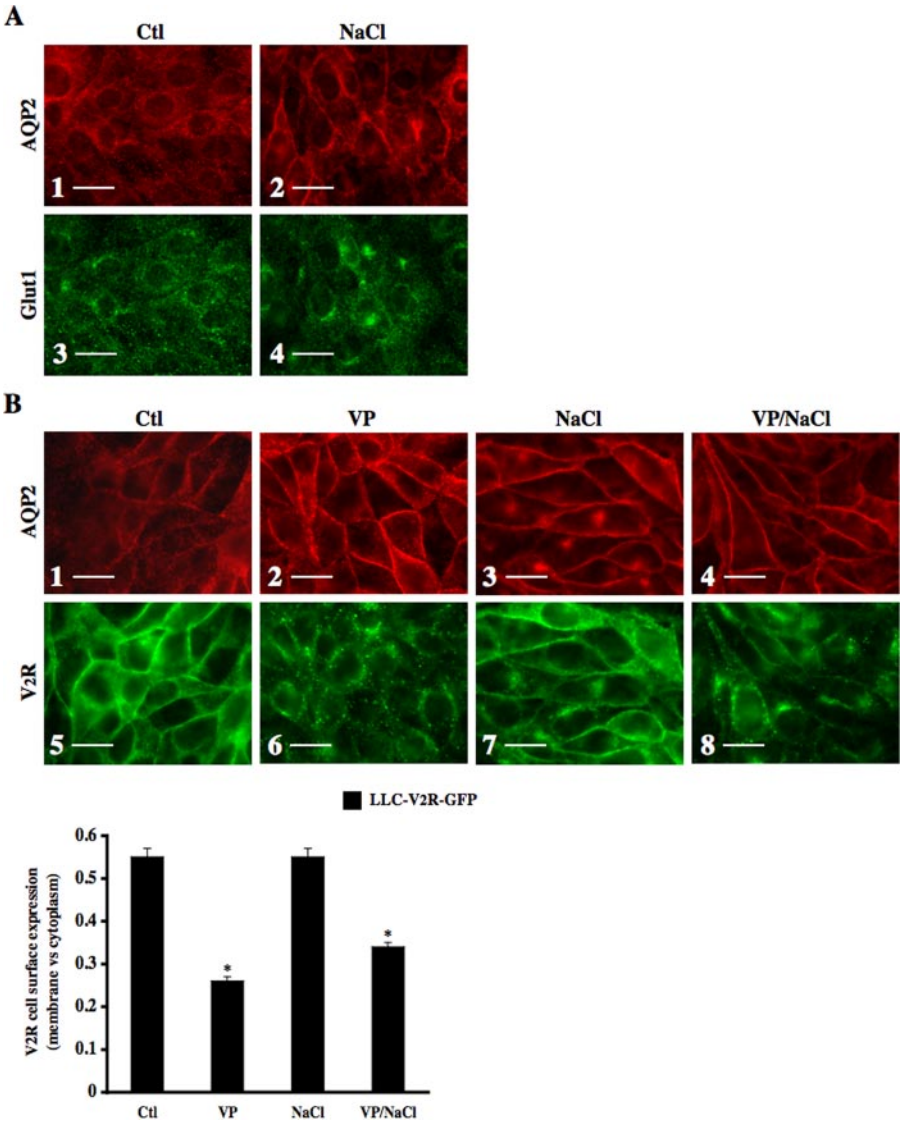

FIGURE 3. **Increased cell surface expression of AQP2 by hypertonicity is not a general phenomenon affecting all plasma membrane-bound proteins.** The effects of hypertonicity on cell surface expression of Glut1 (*A*) and V_2R (*B*) was compared with that of AQP2. *A*, LLC-AQP2 cells were challenged or not (*Ctl*) with NaCl-enriched hypertonic (500 mosmol/kg) medium for 30 min prior to fixation and staining with anti-c-*myc* and anti-Glut1 antibodies for detection of AQP2 (*red*; *1* and *2*) and Glut1 (*green*; *3* and *4*), respectively. Although AQP2 accumulated at both the cell surface and in a perinuclear region following hypertonic challenge (*2*), Glut1 only redistributed to a perinuclear region (*4*). *B*, LLC-V_2R-GFP cells were challenged or not (*Ctl*) with hypertonic medium for 10 min and then for an additional 20 min with or without vasopressin prior to fixation and staining with an anti-c-*myc* antibody for detection of AQP2 (*red*; *1–4*). V_2R expression was detected as a *green* (GFP) signal (*5–8*). In the presence of VP, although hypertonic challenge led to an increase of AQP2 at the cell surface (*4*), V_2R was predominantly expressed in a perinuclear region (*8*). *Bar*, 15 μm. Representative images of three independent experiments are shown. V_2R cell surface expression was determined as described under "Experimental Procedures." Results are mean ± S.E. ($n = 3$). *, $p < 0.05$.

tein (5 μg) were separated by NuPAGE 4–12% BisTris gel (Invitrogen) electrophoresis and transferred to polyvinylidene difluoride membranes (Invitrogen) using an iBlot Gel Transfer apparatus (Invitrogen) set at 20 V for 7 min. Phospho-stress-activated protein kinase/JNK, phospho-p44/42 MAPK, and phospho-p38 MAPK as well as their nonphosphorylated forms were detected by Western blotting using polyclonal rabbit antibodies (Cell Signaling, Danvers, MA) diluted 1:2000. Horseradish peroxidase-conjugated goat anti-rabbit antibody (1:1000) was used as a secondary antibody (Cell Signaling, Danvers, MA). For detection of AQP2, a 1:6 dilution of monoclonal mouse antibody against c-*myc* (30) or a 1:1000 dilution of polyclonal rabbit antibody against a stretch of amino acids corresponding to Glu^{250}-Gln^{263} of the AQP2 C-terminus (for LLC-AQP2 and $mCCD_{cl1}$ cell lysates, respectively) was used. Actin was detected using a monoclonal mouse antibody against actin (1:15,000; Millipore, Billerica, MA). A horseradish peroxidase-conjugated goat anti-mouse antibody (1:5000; Jackson ImmunoResearch) was used against mouse antibodies. The antigen-antibody complexes were detected using SuperSignal West Pico Chemiluminescent horseradish peroxidase substrate (Pierce), and band intensity was quantified using IPLab software.

cAMP Analysis—LLC-AQP2 or $mCCD_{cl1}$ cells were grown to confluence and then incubated in serum- and hormone-free medium as described above prior to 30 min of preincubation in the absence or presence of 1 mM 3-isobutyl-1-methylxanthine (IBMX). Cells were then stimulated with various concentrations of VP or with NaCl-enriched hypertonic medium for an additional 15 min. Cells were then rinsed with PBS and lysed, and cAMP content was measured using the cAMP Biotrack Enzymeimmunoassay system (Amersham Biosciences) following the manufacturer's instructions, as previously described (31).

FITC-Dextran Endocytosis—LLC-AQP2 or $mCCD_{cl1}$ cells were grown to confluence and then incubated in serum- and hormone-free medium as described above. Cells were then continuously stimulated with isotonic (300 mosmol/kg) medium or were subjected to hypertonic (500 mosmol/kg) medium for various periods of time in the presence of 2.5 mg/ml FITC-dextran (Molecular Probes, Inc., Eugene, OR). Cells were then rinsed with PBS, pH 7.4, fixed in PBS containing 4% (w/v) paraformaldehyde and 5% (w/v) sucrose for 20 min, mounted in Vectashield (Vector Laboratories, Burlingame, CA), and examined using a Nikon Eclipse 80i epifluorescence microscope. The pixel intensity of four representative images, taken with a Plan Apo ×40/1.0 numerical aperture Nikon objective, of each experimental condition was determined using IPLab software.

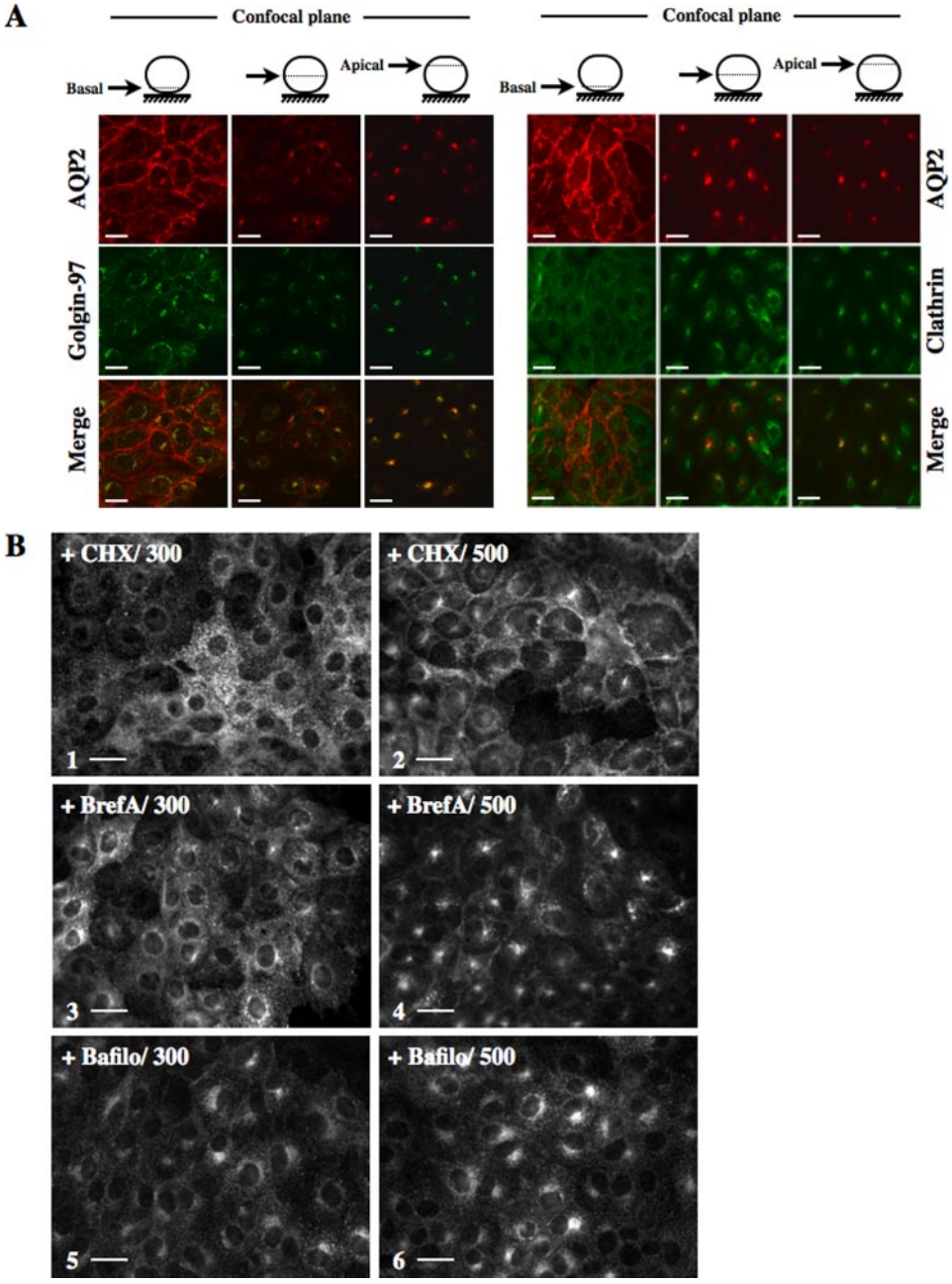

FIGURE 4. **AQP2 accumulates in the trans-Golgi region in response to acute hypertonicity.** *A*, LLC-AQP2 cells were challenged with NaCl-enriched hypertonic (500 mosmol/kg) medium prior to fixation and staining with anti-c-*myc* (for detection of AQP2; *red*) and with either anti-golgin-97 (*green*; *right*) or anti-clathrin (*green*; *left*) antibodies and confocal microscopy imaging. Three focal planes are shown. *B*, LLC-AQP2 cells were pretreated for 30 min with cycloheximide (*CHX*; *1* and *2*) or brefeldin A (*BrefA*; *3* and *4*) and then challenged with isotonic (300 mosmol/kg; *300*) or NaCl-enriched hypertonic (500 mosmol/kg; *500*) medium for an additional 30 min prior to fixation, staining with an anti-c-*myc* antibody, and epifluorescence microscopy analysis. For experiments performed with bafilomycin (*Bafilo*; *5* and *6*), LLC-AQP2 cells were simultaneously challenged with bafilomycin and either isotonic (*300*) or hypertonic (*500*) medium for 30 min prior to fixation, staining with an anti-c-*myc* antibody, and epifluorescence microscopy analysis. *Bar*, 10 μm. Images representative of three independent experiments are shown.

ssYFP Exocytosis—LLC-AQP2 cells were stably transfected with YFP cDNA 5′-flanked by a signal peptide sequence that allows its translocation in the endoplasmic reticulum lumen. The use of ssYFP as a relevant marker of vesicle exocytosis in LLC-PK_1 cells has recently been established (32). Cells were grown in 24-well plates to 90% confluence and then incubated for 1 h in Hanks' buffer supplemented with 20 mM HEPES. The buffer was changed once more (250-μl total volume/well) prior to stimulation or not (control) for various periods of time. 150 μl of cell medium containing secreted YFP from each condition was then collected, and fluorescence was measured using a Beckman Coulter DTX 880 microplate reader (485-nm excitation filter and 535-nm emission filter) and Multimode Detection software (Beckman Coulter, Fullerton, CA).

[^{3}H]VP Binding Assay—[^{3}H]VP binding was performed as previously described (33) on nonstimulated LLC-AQP2 and $mCCD_{cl1}$ cells grown to confluence on Transwell® filters (10^6 LLC-AQP2 cells/filter and 3.2×10^6 $mCCD_{cl1}$ cells/filter). The culture medium was replaced by ice-cold PBS, and 16 nM [^{3}H-8-arginine]vasopressin (PerkinElmer Life Sciences) was added to the upper or lower chamber to determine either apical (upper chamber) or basolateral (lower chamber) [^{3}H]VP binding. Incubation was carried out for 3 h at 4 °C. Nonspecific binding was determined in the presence of excess unlabeled VP (1 μM). Cells were then rinsed twice with ice-cold PBS, after which the filters were excised and solubilized in scintillation vials containing 500 μl of NaOH (0.1 N). After 12 h, 5 ml of Optic-Fluor scintillation fluid (Packard, Groningen, The Netherlands) was added, and bound radioactivity was determined using a Tricarb 2200 CA liquid scintillation analyzer (Packard). Data from three experiments were analyzed.

Image Semiquantification—AQP2 expression at the proximity of the plasma membrane was semiquantified as previously described (20) using IPLab software. Briefly, the number of pixels contained in an outline enclosing the plasma membrane or the cell cytoplasm was quantified as integrated optical density (IOD) values. The plasma membrane/cell cytoplasm sorting index is defined as the IOD of the plasma membrane divided by the cytoplasmic IOD. At least 45 cells from at least three independent experiments were analyzed for each experimental condition, and the mean plasma membrane/cell cytoplasm sorting index ± S.E. was determined. We compared the number of pixels contained

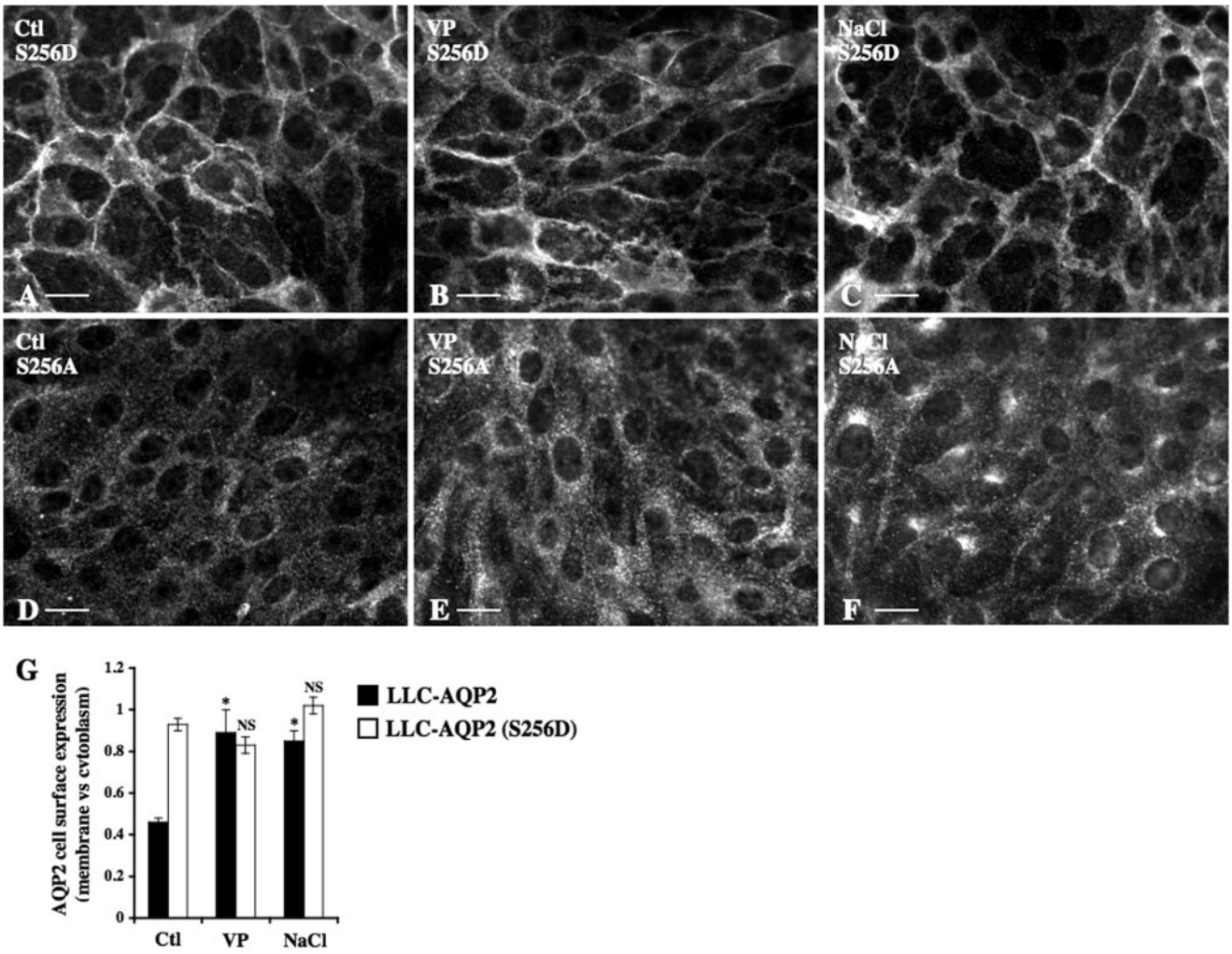

FIGURE 5. **Acute hypertonicity induces segregation of Ser^{256} phosphorylated and nonphosphorylated AQP2 into separate compartments.** LLC-AQP2 (S256D) (*A–C*), LLC-AQP2 (S256A) (*D–F*), or LLC-AQP2 cells (quantified in *G*) were challenged or not (*Ctl*) for 30 min with either NaCl-enriched hypertonic (500 mosmol/kg) medium or VP prior to fixation and staining with an anti-c-*myc* antibody. *Bar*, 10 μm. *G*, AQP2 cell surface expression was determined as described under "Experimental Procedures." Results are mean ± S.E. ($n = 5$). *, $p < 0.05$. *NS*, not significant.

in a same intracellular surface of LLC-AQP2 (S256A) cells subjected to isotonic conditions or to 30 min of hypertonic (500 mosmol/kg) challenge. Semiquantification analysis of 40 cells from each group revealed similar IOD values ($p < 0.05$), indicating that pixel quantification is similar between cells that do or do not display a hypertonicity-induced accumulation of perinuclear AQP2. This in turn indicates that a measured increase of wild-type AQP2 expression in the proximity of the plasma membrane under hypertonic conditions is not due to an underestimation of cytoplasmic AQP2 expression but rather reflects an accumulation of AQP2 at or near the cell surface.

As shown in Fig. 2, increased AQP2 expression in the proximity of the plasma membrane was accompanied by increased AQP2 expression at the cell surface in response to acute hypertonic challenge. For the sake of simplicity, we will refer to a shift of AQP2 expression toward the cell surface simply as an increase of AQP2 cell surface expression.

Statistics—Results are given as the mean ± S.E. from *n* independent experiments. Each experiment was performed on cells from the same passage. Statistical differences were assessed using the Mann-Whitney *U* test or the Kruskal-Wallis test for comparison of two groups or more, respectively. A value of $p < 0.05$ (*) was considered significant. **, $p < 0.01$.

RESULTS

Acute Hypertonicity Increases AQP2 Expression at the Plasma Membrane—Cultured mCCD$_{cl1}$ cells that express endogenous AQP2 and LLC-AQP2 cells stably transfected with AQP2 were used as models for investigation of AQP2 trafficking following VP challenge or hypertonic stimulation. A [^{3}H]VP binding assay performed on both cell lines revealed that although V_2R is evenly distributed between the basal and apical sides of LLC-PK1 cells (45.4 ± 5.8 and 54.6 ± 27.1%) as previously described (33), V2R is predominantly expressed at the basal side of mCCD$_{cl1}$ cells (86.8 ± 4 and 13.2 ± 2.4% basal and apical expression, respectively). Moreover, VP similarly increased AQP2 cell surface expression in LLC-PK1 cells grown either on glass coverslips or permeable filters. On the other hand, VP only increased AQP2 cell surface expression in mCCD$_{cl1}$ cells grown on filters and only when added to the basal medium. This led us

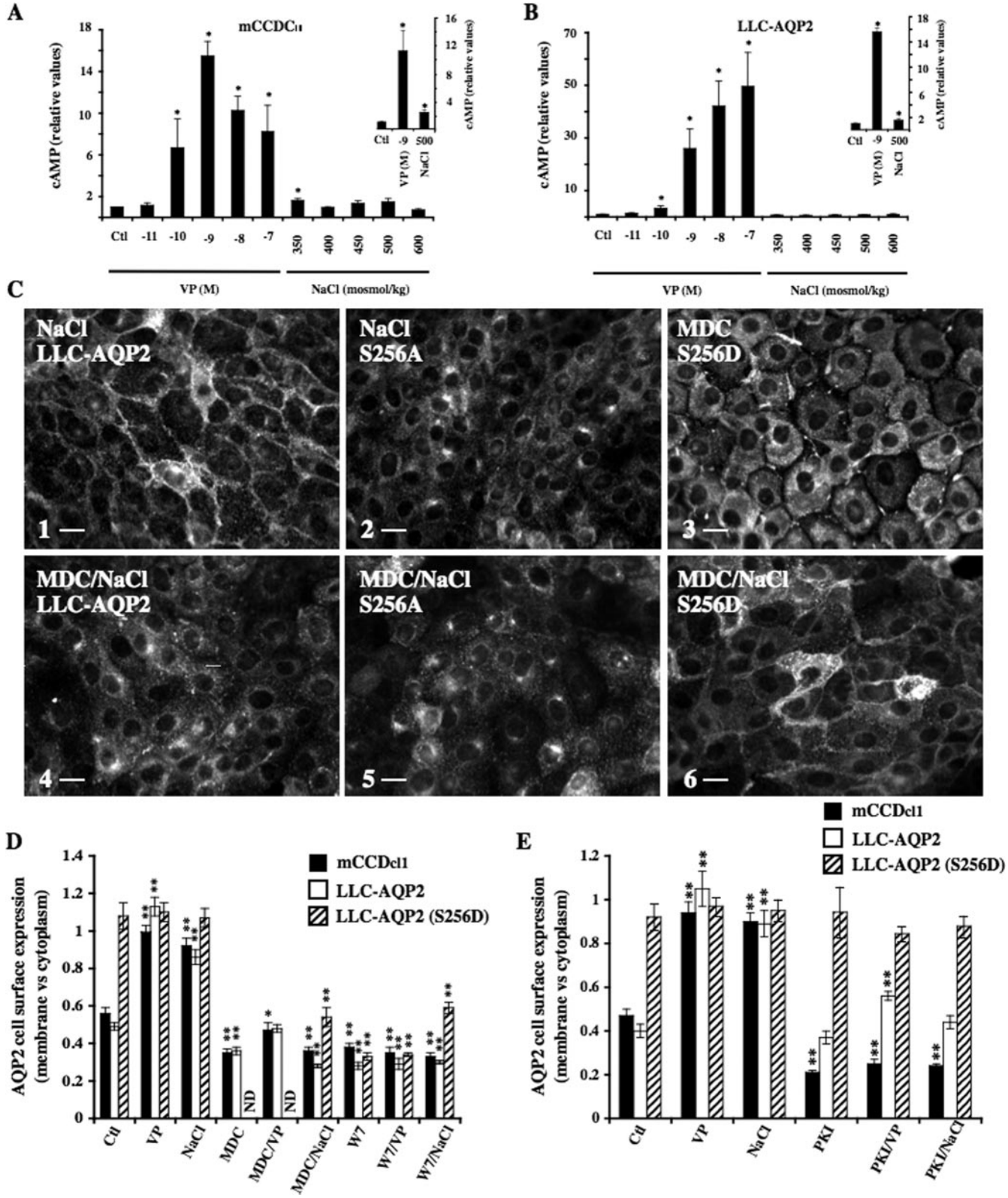

FIGURE 6. **AQP2 accumulation at the cell surface following acute hypertonicity occurs independently of a rise of cAMP concentration.** MCCDcl$_1$ cells (*A*) and LLC-AQP2 cells (*B*) were preincubated or not for 30 min with IBMX and challenged or not (*Ctl*) for 30 min with either NaCl-enriched hypertonic (350–600 mosmol/kg) medium or various concentrations of VP prior to cell lysis and determination of cAMP concentration. The ratio of cAMP concentration measured for each experimental condition and that measured in nonstimulated (*Ctl*) cells, in the absence and presence (*inset*) of IBMX, is shown. Results are mean ± S.E. ($n = 4$). *, $p < 0.05$. *C–E*, mCCDc$_{l1}$, LLC-AQP2, LLC-AQP2 (S256D), and LLC-AQP2 (S256A) cells were preincubated or not for 5 min with calmodulin inhibitors MDC or W-7 and then challenged or not (*Ctl*) for 30 min with either NaCl-enriched hypertonic (500 mosmol/kg) medium or VP prior to fixation and staining with anti-c-*myc* (for LLC-PK$_1$ cells) or anti-AQP2 (for mCCDcl$_1$ cells) antibodies. *C*, representative immunofluorescent images of LLC-AQP2 (*1* and *4*), LLC-AQP2 (S256A) (*2* and *5*), and LLC-AQP2 (S256D) cells (*3* and *6*) depicting the effects of MDC on AQP2 trafficking under hypertonic conditions. *Bar*, 10 μm. *D* and *E*, AQP2 cell surface expression was determined as described under "Experimental Procedures." Results are mean ± S.E. ($n = 4$). *ND*, not determined. *, $p < 0.05$; **, $p < 0.01$.

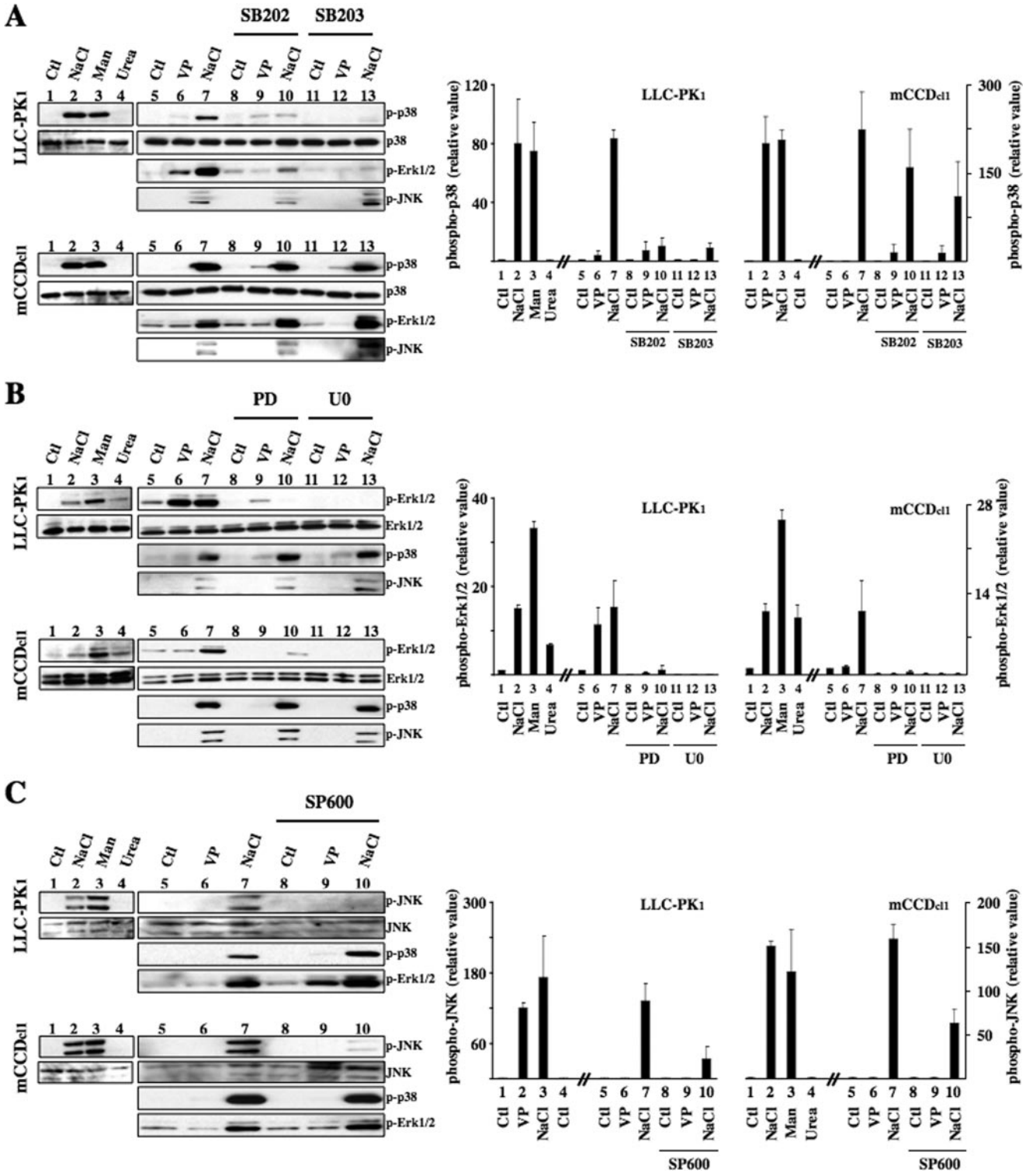

FIGURE 7. **Effect of MAPK pharmacological inhibitors on hypertonicity-induced MAPK activity.** mCCDc$_{l1}$ and LLC-AQP2 cells were preincubated or not 30 min with p38 MAPK inhibitors SB 202190 (*SB202*) or SB 203580 (*SB203*) (*A*), with MEK-1 and -2 inhibitors PD 98059 or U0126 (*B*), or with the JNK inhibitor SP600125 (*SP600*) (*C*) and then challenged or not (*Ctl*) for 30 min with either NaCl- or mannitol-hypertonic (500 mosmol/kg) medium, with urea-hyperosmotic (500 mosmol/kg) medium or with VP. Cells were lysed, and total protein extracts were separated by SDS-PAGE, and phospho-p38 MAPK, phospho-ERK1/2 MAPK, and phospho-JNK MAPK as well as their nonphosphorylated forms were detected by Western blot using polyclonal antibodies. Representative immunoblots are shown. Densitometric quantification of phosphorylated MAPKs expressed as the ratio of optical density values measured for each experimental condition *versus* nonstimulated (*Ctl*, *lane 1*) cells is shown. Results are mean ± S.E. ($n = 3$).

to conduct our investigations on LLC-PK1 cells grown on glass coverslips and on mCCD$_{cl1}$ cells grown on permeable filters.

AQP2 cell surface expression following 30 min of VP or NaCl-induced hypertonic stimulation was compared by immunofluorescence analysis and image semiquantification in LLC-

AQP2 cells, $mCCD_{cl1}$ cells, and Brattleboro rat kidney slices (Figs. 1 and 2). In all three models, AQP2 accumulated at the plasma membrane to a similar extent in response to 30 min of hypertonic challenge (500 mosmol/kg for cultured cells and 1000 mosmol/kg for kidney slices; Fig. 1, *B*, *E*, and *H*) or 10 nM VP stimulation (Fig. 1, *C*, *F*, and *I*), as compared with nonstimulated cells maintained in isotonic (300 mosmol/kg) medium (control; Fig. 1, *A*, *D*, and *G*). Increased AQP2 plasma membrane expression in response to 30 min of hypertonic (500 mosmol/kg) challenge was also observed in MDCK-AQP2 cells (increased expression as compared with control cells standardized to 1: 1.96 ± 0.03 for hypertonic stimulation, 3.39 ± 0.07 for 10 μM forskolin stimulation). As a control for nonspecific binding of secondary antibody, experiments performed in the absence of primary antibody produced a small background signal that was not affected by either VP or hypertonicity (not shown). Immunofluorescence analysis of kidney slices (Fig. 1, *G–I*) further revealed that increased AQP2 expression at the plasma membrane in response to acute hypertonicity was mostly restricted to the apical side of principal cells of the proximal and distal inner medullary CD, whereas VP led to an accumulation of AQP2 at both apical and basal plasma membranes, as previously reported (20) (ratio of apical/basal AQP2 cell surface expression as revealed by image semiquantification: control, 0.89 ± 0.09; NaCl, 3.83 ± 0.33; VP, 1.69 ± 0.21). Semiquantification of images revealed that increased AQP2 expression at the proximity of the plasma membrane induced by NaCl-hypertonic stimulation returned to base-line levels 30 min after cells were returned to isotonic medium (Fig. 2, *B* and *C*). The extent of increased AQP2 expression at the plasma membrane of LLC-AQP2 and $mCCD_{cl1}$ cells following 10 min of hypertonic (500 mosmol/kg) stimulation was similar to that observed following 30 min of

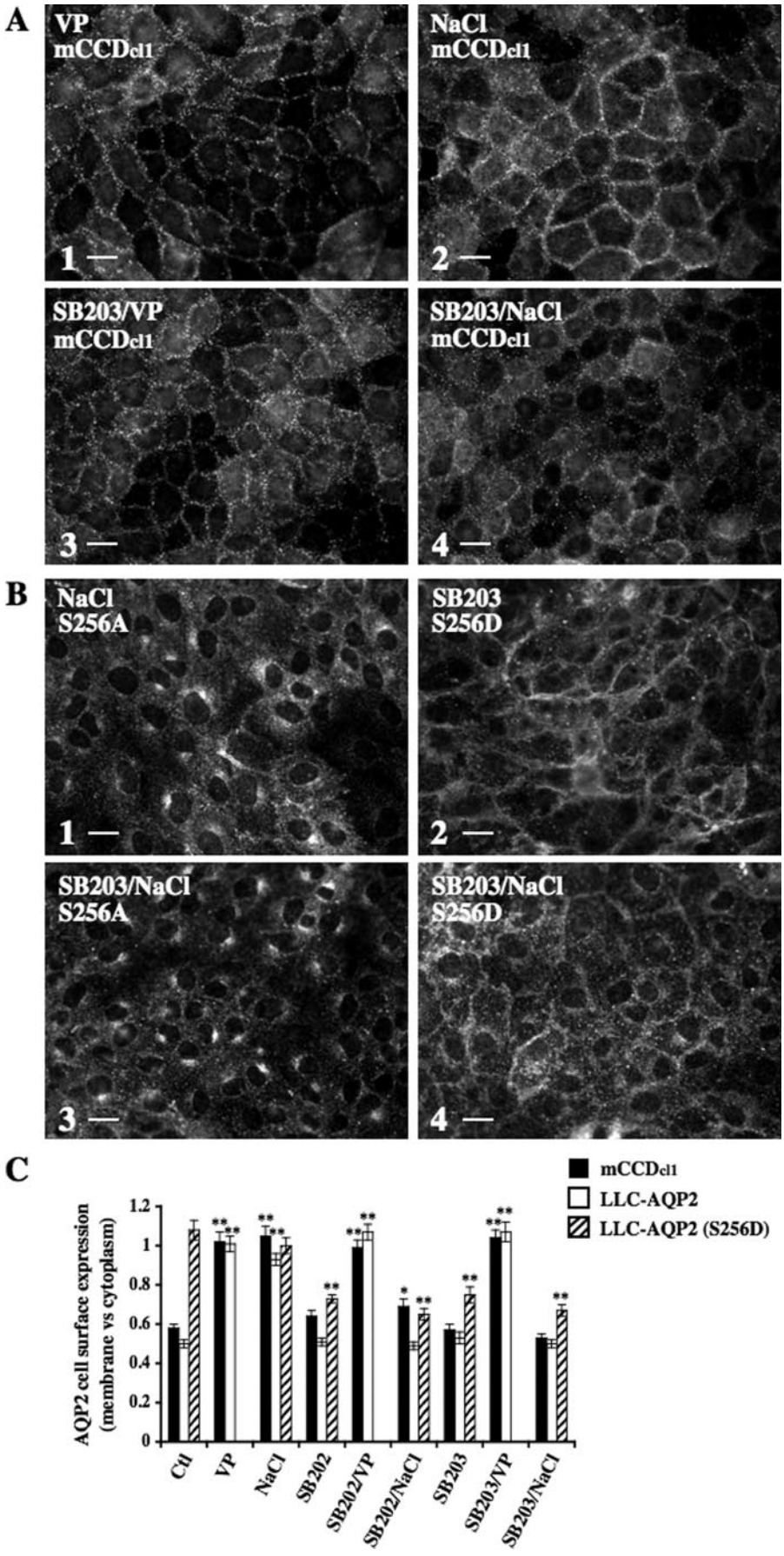

hypertonic stimulation (Fig. 2*B*). AQP2 apical expression observed in kidney slices, on the other hand, was greatest following 10 min of hypertonic (1000 mosmol/kg) stimulation (Fig. 2*C*), indicating that AQP2 accumulation at the plasma membrane in response to hypertonicity is more transient in the slice preparation. The effect of hypertonicity was reproduced in cells challenged for 30 min with only 350 mosmol/kg (for LLC-AQP2 and $mCCD_{cl1}$ cells) or 600 mosmol/kg (for kidney slices) NaCl-enriched medium (Fig. 2, *B* and *C*). Similar levels of AQP2 expression at the cell surface were observed after 30 min of exposure to mannitol-enriched hypertonic (500 mosmol/kg for cultured cells and 1000 mosmol/kg for kidney slices) medium, whereas 30 min of urea-hyperosmotic (500 mosmol/kg) stimulation did not affect AQP2 plasma membrane expression (Fig. 2, *B* and *C*). We next tested whether hypertonicity increases apical AQP2 expression in cultured cells, as observed in kidney slices (Fig. 2*D*). *x-z* scans of images acquired by confocal microscopy revealed that whereas VP stimulation increased AQP2 expression at the lateral surface of LLC-PK1 cells, hypertonicity increased AQP2 expression at both apical and lateral surfaces. Similarly, hypertonicity induced a strong shift of AQP2 expression toward the apical pole of $mCCD_{cl1}$ cells. Increased AQP2 cell surface expression was not due to an increase of AQP2 abundance, since 30 min of hypertonic stimulation did not alter AQP2 whole cell levels in either cell line (Fig. 2*E*; as compared with control cells standardized to 1: 1.07 ± 0.13 and 0.97 ± 0.05 for LCC-AQP2 and $mCCD_{cl1}$ cells, respectively). Observations made by *x-z* analysis of confocal images are supported by results of Western blot analysis of biotinylated cell surface proteins precipitated with streptavidin-agarose (Fig. 2*E*). Indeed, the intensity of a 28 kDa band corresponding to AQP2 protein, absent in cells that were not incubated with biotin, significantly increased in LLC-AQP2 cells after 30 min of hypertonic (500 mosmol/kg) challenge (increased expression as compared with control cells standardized to 1: 5.1 ± 1.6 for hypertonic stimulation, 2.5 ± 0.5 for 10 nM VP stimulation). These observations collectively indicate that a small increase in environmental tonicity induces a rapid, transient, and reversible increase of AQP2 expression toward the apical and lateral sides of challenged cells.

In order to test the specificity of the effect of hypertonicity on increased AQP2 cell surface expression, we investigated whether hypertonicity induces a similar shift of Glut1 and/or V_2R trafficking in LLC-AQP2 cells (Fig. 3). Although AQP2 and Glut1 expression was mostly intracellular in nonstimulated cells, 30 min of hypertonic challenge only increased AQP2 cell surface expression (Fig. 3*A*). As previously demonstrated (27), V_2R is abundantly expressed at the cell surface of nonstimulated cells and is internalized after 30 min of 1 μM VP stimulation (Fig. 3*B*, compare *5* and *6*). Hypertonicity (500 mosmol/kg) had no significant effect on V_2R cell surface expression in the absence of VP (Fig. 3*B*, compare *5* and *7*) and only slightly reduced VP-induced V_2R internalization (compare *6* and *8*). As discussed below, in addition to increased AQP2 expression at the plasma membrane, hypertonicity but not VP induced an accumulation of AQP2 in a perinuclear compartment. This was especially apparent in LLC-AQP2 cells challenged for 30 min with hypertonic medium (Fig. 1), although significant perinuclear staining was detectable even after just 10 min of stimulation. Interestingly, hypertonicity induced a similar perinuclear accumulation of both Glut1 (Fig. 3*A*, *4*) and V_2R (Fig. 3*B*, *7* and *8*). Taken together, these observations indicate that the effects of hypertonicity on AQP2 cell surface expression are not a generalized phenomenon affecting all plasma membrane-bound proteins.

Acute Hypertonicity Induces Segregation of Ser^{256}-phosphorylated and -nonphosphorylated AQP2 into Separate Compartments—AQP2 perinuclear accumulation following hypertonic challenge observed in the present study was previously observed in LLC-AQP2 cells exposed to low temperature or treated with bafilomycin (34). In that study, the perinuclear compartment was identified as the *trans*-Golgi network (TGN). This led us to investigate whether hypertonicity induces AQP2 accumulation in the TGN by performing confocal microscopy on LLC-AQP2 cells subjected to 30 min of hypertonic challenge and doubly labeled against AQP2 and golgin-97, a peripheral membrane protein localized at the TGN (Fig. 4*A*, *left*), or against AQP2 and clathrin (Fig. 4*A*, *right*). Clathrin is concentrated in transport vesicles derived from the plasma membrane and the TGN (35, 36) and can be used as a TGN marker (34, 35), although a subpopulation of recycling endosomes also consists of clathrin-coated vesicles (37). Confocal imaging of the basal side of cells revealed that, under hypertonic conditions, whereas AQP2 (*red*) was concentrated at the proximity of the plasma membrane, golgin-97 (*green*) was predominantly perinuclear. Clathrin (*green*) was present in a diffuse, punctate distribution, as expected (Fig. 4*A*, *left*). When confocal images were collected from more apical regions of the cell, strong perinuclear staining was observed for AQP2, golgin-97, and clathrin (Fig. 4*A*, *center* and *right*). Merged images revealed a partial overlap (*yellow*) of AQP2 with both golgin-97 and clathrin, indicating that AQP2 rapidly accumulates in a golgin-97- and clathrin-positive region (*trans*-Golgi) of the cell following hypertonic challenge. Next, we investigated the subcellular origin of AQP2 that accumulates in the *trans*-Golgi region following hypertonic challenge (Fig. 4*B*). LLC-AQP2 cells were first treated for 20 min with either 20 μM cycloheximide (Fig. 4*B*, *1* and *2*), a protein synthesis inhibitor, or 7 μM brefeldin A (Fig. 4*B*, *3* and *4*), which blocks translocation of proteins from the endoplasmic reticulum to the Golgi apparatus, prior to 30 min of hypertonic (500 mosmol/kg) challenge. Neither compound decreased hypertonicity-induced AQP2 perinuclear staining,

FIGURE 8. **AQP2 accumulation at the cell surface, but not the *trans*-Golgi region, following acute hypertonicity depends on p38 MAPK activity.** $mCCDc_{l1}$, LLC-AQP2, LLC-AQP2 (S256D), and LLC-AQP2 (S256A) cells were preincubated or not for 30 min with p38 MAPK inhibitors SB 202190 (SB202) or SB 203580 (SB203) and then challenged or not (*Ctl*) for 30 min with either NaCl-enriched hypertonic (500 mosmol/kg) medium or VP. Cells were fixed and stained with anti-c-*myc* (for LLC-PK_1 cells) or anti-AQP2 (for $mCCDcl_1$ cells) antibodies for analysis of AQP2 expression at the cell surface and *trans*-Golgi region. Representative immunofluorescent images of $mCCDc_{l1}$ (*A*), LLC-AQP2 (S256A) (*B*; *1* and *3*) and LLC-AQP2 (S256D) cells (*B*; *2* and *4*) depicting the effects of SB 203580 on AQP2 trafficking under hypertonic conditions are shown. *Bar*, 7 μm (*A*) and 10 μm (*B*). *C*, AQP2 cell surface expression was determined as described under "Experimental Procedures." Results are mean $\pm$ S.E. ($n = 4$). *, $p < 0.05$; **, $p < 0.01$.

suggesting that recycling AQP2 rather than newly synthesized protein is the major contributor to the formation of the perinuclear, TGN-associated patch following hypertonic challenge.

Constitutive AQP2 recycling between the plasma membrane and the *trans*-Golgi region was previously revealed in LLC-AQP2 cells by treating cells with bafilomycin, an H^+-ATPase inhibitor reported to perturb intracellular trafficking (34). We investigated the effect of bafilomycin on hypertonicity-induced AQP2 cell surface accumulation by subjecting cells to isotonic or hypertonic (500 mosmol/kg) medium for 30 min in the presence of 125 nM bafilomycin (Fig. 4*B*, *5* and *6*). Under isotonic conditions, bafilomycin treatment induced an accumulation of AQP2 at the *trans*-Golgi region that was even more prominent under hypertonic conditions. Importantly, bafilomycin additionally abolished hypertonicity-induced AQP2 accumulation at the cell surface, suggesting that AQP2 constitutively recycles between the plasma membrane and the *trans*-Golgi region under hypertonic conditions. Bafilomycin-induced accumulation of AQP2 at the *trans*-Golgi region was previously shown to be unaffected by VP stimulation (34). Interestingly, 10 nM VP greatly reduced the hypertonicity-induced (500 mosmol/kg) accumulation of AQP2 at the *trans*-Golgi region (Fig. 4*B*, compare *3* and *4*), revealing that this effect of hypertonicity can be reversed by VP stimulation, possibly by redirecting AQP2 from the *trans*-Golgi region to the plasma membrane.

Phosphorylation of AQP2 at Ser^{256} is essential but not sufficient for steady-state expression of AQP2 at the cell surface (10, 12, 25, 38). We investigated the Ser^{256} phosphorylation state of AQP2 that accumulates at the cell surface and in the *trans*-Golgi region following hypertonic challenge by comparing hypertonicity-induced accumulation of AQP2 in both regions of LLC-PK_1 cells stably expressing

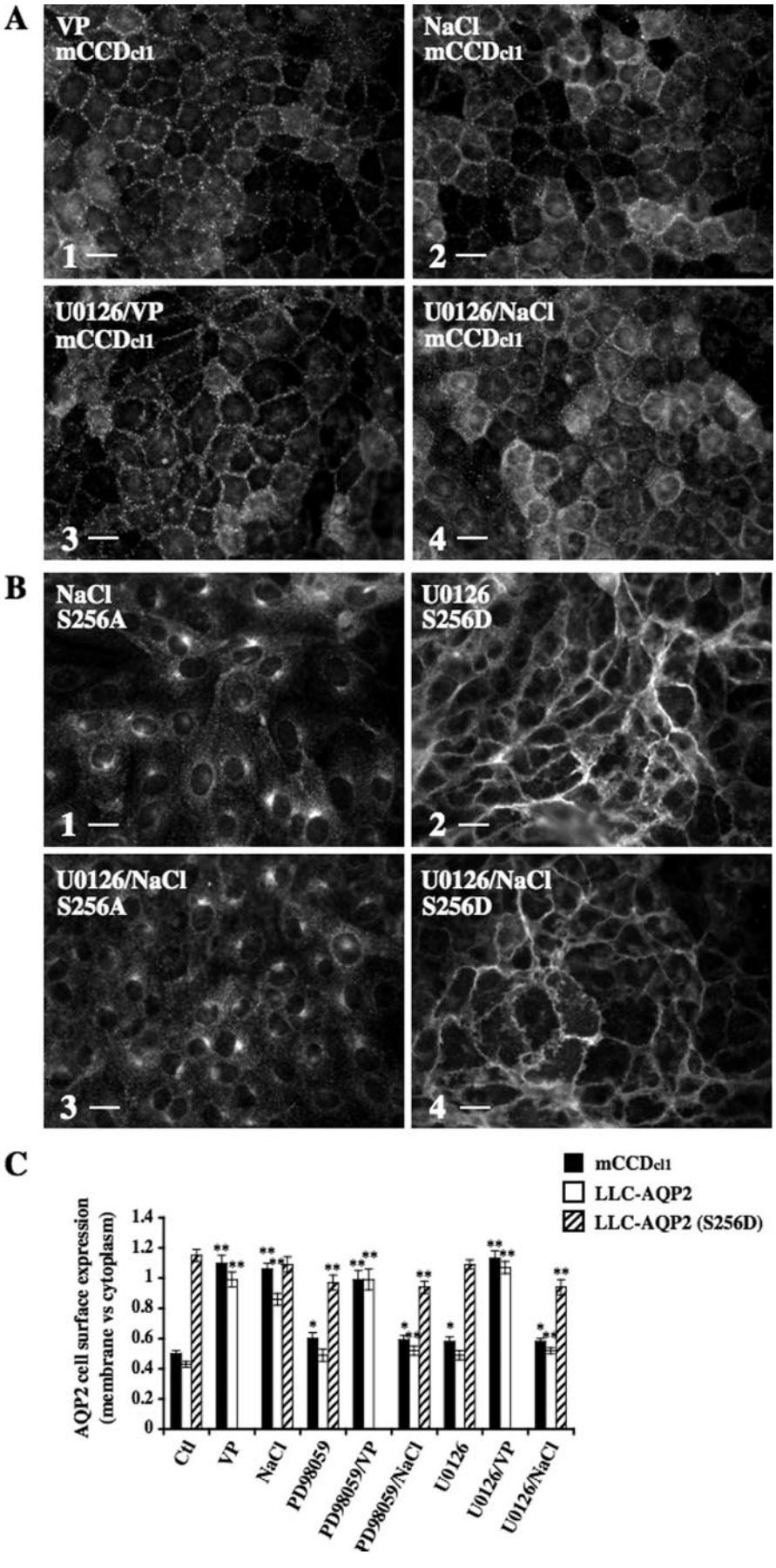

mutants that either mimic Ser^{256}-phosphorylated (LLC-AQP2 (S256D)) or nonphosphorylated (LLC-AQP2 (S256A)) AQP2 (Fig. 5). Immunofluorescence imaging revealed that about 50% of AQP2 in LLC-AQP2 (S256D) cells resided in the plasma membrane under isotonic (300 mosmol/kg) conditions (Fig. 5, *A* and *G*) and that AQP2 cell surface expression was not further increased by either 10 nM VP or hypertonicity (500 mosmol/kg) after 30 min of stimulation (Fig. 5, *B*, *C*, and *G*). Neither VP nor hypertonic challenge increased AQP2 expression at the plasma membrane of LLC-AQP2 (S256A) cells (Fig. 5, *D–F*), whereas hypertonicity, but not VP, induced a perinuclear accumulation of AQP2 in LLC-AQP2 (S256A) cells that was comparable with that observed for wild-type AQP2 (see Fig. 1*B*). These observations collectively indicate that AQP2 residing in the plasma membrane of hypertonicity-challenged cells consists of Ser^{256} phosphorylated AQP2, whereas nonphosphorylated AQP2 accumulates in the *trans*-Golgi region.

Increased AQP2 Expression at the Cell Surface and trans-Golgi Region in Response to Acute Hypertonicity Occurs Independently of an Increase of cAMP Concentration—The effects of hypertonicity and VP on cAMP intracellular concentration were compared in $mCCD_{cl1}$ and LLC-AQP2 cells by subjecting cells to various concentrations of VP or to medium of increasing tonicity for 15 min (Fig. 6, *A* and *B*). cAMP concentration significantly ($p < 0.05$) increased following 100 pM VP stimulation and increased to greater extents at higher doses of VP. Hypertonicity, on the other hand, did not produce an increase of cAMP concentration, although a small, but significant, increase was observed in cells pretreated with 100 μM IBMX, an inhibitor of cAMP phosphodiesterase (Fig. 6, *A* and *B*, *inset*). Several pieces of evidence suggest that calmodulin-sensitive adenylyl cyclase type 3 plays an important role in mediating the AVP-induced increase of intracellular cAMP (39). Accordingly, calmodulin inhibition blocked VP-induced redistribution of AQP2 toward the cell surface, at least partly by attenuating adenylyl cyclase-mediated cAMP elevation (39). We further investigated the influence of cAMP concentration on hypertonicity-induced altered AQP2 trafficking by treating $mCCD_{cl1}$ and LLC-AQP2 cells with either of two different calmodulin inhibitors (200 μM monodansylcadaverine (MDC) and 25 μM W-7; EMD Biosciences, La Jolla, CA) (Fig. 6, *C* and *D*). Both compounds significantly attenuated the increase of cAMP concentration induced by 30 min of 10 nM VP stimulation (cAMP concentration as compared with VP-stimulated cells standardized to 1: 0.27 ± 0.02 for MDC and 0.34 ± 0.06 for W-7 in $mCCD_{cl1}$ cells and 0.36 ± 0.06 for MDC and 0.63 ± 0.01 for W-7 in LLC-AQP2 cells). Pretreatment of either cell line with either compound abolished the increase of wild-type AQP2 at the cell surface induced by 30 min of either 10 nM VP (Fig. 6*D*) or hypertonic (500 mosmol/kg; Fig. 6, *C* and *D*) stimulation. Interestingly, the base-line cell surface expression of AQP2 in LLC-AQP2 (S256D) cells was also either abolished or greatly reduced in cells treated with either MDC or W-7, respectively. Hypertonicity, but not VP, partially restored AQP2 expression at the surface of LLC-AQP2 (S256D) cells (Fig. 6, *C*, *3* and *6*, and *D*). Hypertonicity-induced accumulation of AQP2 in the *trans*-Golgi region of either LLC-AQP2 or LLC-AQP2 (S256A) cells was not visibly affected by either MDC or W-7 (Fig. 6*C*, *2* and *5*). In agreement with observations made in LLC-AQP2 (S256D) and LLC-AQP2 (S256A) cells (Fig. 5), immunofluorescence imaging revealed that 10 μM PKI (EMD Biosciences, La Jolla, CA), a myristoylated PKA inhibitor, abolished (for $mCCD_{cl1}$ cells) or reduced (for LLC-AQP2 cells) AQP2 expression at the cell surface induced by 30 min of either 10 nM VP or hypertonic (500 mosmol/kg) stimulation (Fig. 6*E*). Similar to MDC and W-7, hypertonicity-induced accumulation of AQP2 in the *trans*-Golgi region of LLC-AQP2 and LLC-AQP2 (S256A) cells was not visibly affected by PKI (data not shown). Contrary to the effect produced by calmodulin inhibition (Fig. 6*D*), PKI did not affect AQP2 cell surface expression in LLC-AQP2 (S256D) cells (Fig. 6*E*). Collectively, these results suggest that increased AQP2 expression at the cell surface and in the *trans*-Golgi region following hypertonic challenge is not mediated by alterations of cAMP concentration but that the hypertonicity-induced increase of AQP2 expression at the cell surface does depend on PKA activity and on AQP2 phosphorylation at Ser^{256}.

Increased AQP2 Expression at the Cell Surface in Response to Acute Hypertonicity Depends on p38, ERK, and JNK MAPK Signaling—In renal cells, three major kinases activated by hypertonicity are p38, ERK, and JNK MAPKs (5). In the present study, we investigated the role that these kinases may play in hypertonicity-induced AQP2 trafficking. Western blot analysis of phosphorylated p38 (Fig. 7*A*), phosphorylated ERK1/2 (Fig. 7*B*), and phosphorylated JNK (Fig. 7*C*) showed that both $mCCD_{cl1}$ and LLC-AQP2 cells displayed increased levels of p38 and JNK activity in response to 30 min of NaCl- or mannitol-hypertonic (500 mosmol/kg) but not urea-hyperosmotic (500 mosmol/kg) challenge. Similarly, ERK1/2 activity was increased by 30 min of NaCl- or mannitol-hypertonic challenge but was additionally increased by 30 min of urea-hyperosmotic challenge. Contrary to the effect produced by hypertonicity, 30 min of 10 nM VP stimulation did not increase MAPK phosphorylation levels with the exception of a variable increase of ERK1/2 phosphorylation occurring in LLC-AQP2 cells. We investigated the influence of p38, ERK1/2, and JNK on hypertonicity-induced altered AQP2 trafficking by pharmacological inhibition of MAPK activity. For this purpose, we used two inhibitors of p38 MAPK (SB 202190 and SB 203580; EMD Biosciences, La Jolla, CA), two inhibitors of MAPK kinase (MEK)-1 and -2 (PD 98059 and U0126; EMD Biosciences) that subsequently block ERK phosphorylation/activation, and an inhibitor of JNK1 to -3

FIGURE 9. **AQP2 accumulation at the cell surface, but not the *trans*-Golgi region, following acute hypertonicity depends on ERK1/2 MAPK activity.** $mCCDc_{l1}$, LLC-AQP2, LLC-AQP2 (S256D), and LLC-AQP2 (S256A) cells were preincubated or not for 30 min with MEK-1 and -2 inhibitors PD 98059 or U0126 and then challenged or not (*Ctl*) for 30 min with either NaCl-enriched hypertonic (500 mosmol/kg) medium or VP. Cells were fixed and stained with anti-c-*myc* (for $LLC\text{-}PK_1$ cells) or anti-AQP2 (for $mCCDcl_1$ cells) for analysis of AQP2 expression at the cell surface and *trans*-Golgi region. Representative immunofluorescent images of $mCCDc_{l1}$ (*A*), LLC-AQP2 (S256A) (*B*; *1* and *3*), and LLC-AQP2 (S256D) cells (*B*; *2* and *4*) depicting the effects of U0126 on AQP2 trafficking under hypertonic conditions are shown. *Bar*, 7 μm (*A*) and 10 μm (*B*). *C*, AQP2 cell surface expression was determined as described under "Experimental Procedures." Results are mean ± S.E. ($n = 4$). *, $p < 0.05$; **, $p < 0.01$.

kinases (SP600125; EMD Biosciences). Western blot analysis of $mCCD_{cl1}$ cell lysates revealed that a 10 μM concentration of each pharmacological inhibitor specifically reduced the phosphorylation levels of their respective MAPK targets (although targeted inhibition of p38 phosphorylation was not as great as those observed for ERK1/2 and JNK phosphorylation), demonstrating the specificity of all inhibitors used at 10 μM in $mCCD_{cl1}$ cells. Western blot analysis of LLC-AQP2 cell lysates, on the other hand, revealed inhibitor-specific targeting of JNK (in cells treated with 10 μM SP600125) and ERK1/2 (in cells treated with 2 μM PD 98059 or 1 μM U0126) but not p38 MAPK, since cells treated with 3–10 μM SB 202190 or SB 203580 displayed reduced phosphorylation levels of both p38 and ERK1/2 kinases. Reducing the concentration of ERK1/2 inhibitors below 3 μM reduced their inhibitory effect on ERK1/2 phosphorylation and did not improve their targeting specificity (data not shown). Possibly, this may reflect a cross-talk occurring between p38 and ERK1/2 MAPK pathways in LLC-AQP2 cells. Immunofluorescence imaging revealed that p38, ERK1/2, or JNK inhibitors applied alone all significantly reduced the increase of AQP2 expression at the plasma membrane induced by hypertonicity in both $mCCD_{cl1}$ and LLC-AQP2 cells but had no effect on AQP2 cell surface expression in cells maintained in isotonic (300 mosmol/kg) medium or stimulated with VP (Figs. 8–10). Although inhibition of either ERK1/2 or JNK activity had no effect on AQP2 expression at the cell surface of LLC-AQP2 (S256D) cells (Figs. 9*B* and 10*B*, *2* and *4*, and Figs. 9*C* and 10*C*), inhibition of p38 activity decreased AQP2 cell surface expression in LLC-AQP2 (S256D) cells maintained in isotonic medium or challenged with hypertonic medium (Fig. 8, *B* (*2* and *4*) and *C*). Finally, accumulation of AQP2 in the *trans*-Golgi region of LLC-AQP2 and LLC-AQP2 (S256A) cells

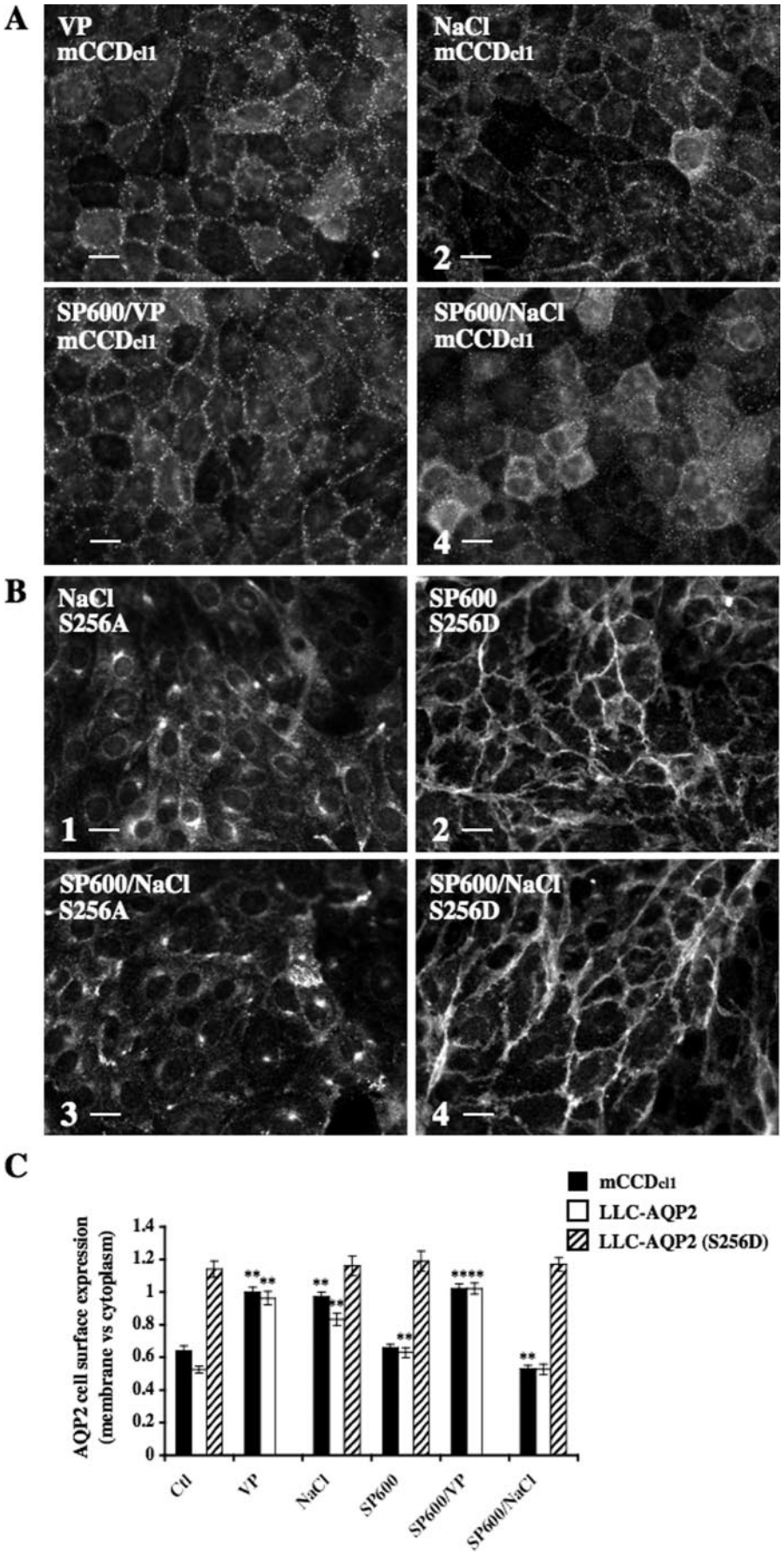

following hypertonic challenge was not visibly altered by MAPK inhibition (Figs. 8*B*, 9*B*, and 10*B*, *1* and *3*, and Figs. 8*C*, 9*C*, and 10*C*). Taken together, these results reveal that simultaneous activation of p38, ERK1/2, and JNK by hypertonicity is required for increased AQP2 expression at the cell surface but not the *trans*-Golgi region immediately following hypertonic challenge. In contrast, inhibition of these kinases had no detectable effect on VP-induced AQP2 accumulation at the cell surface.

Acute Hypertonicity Reduces both Endocytotic and Exocytotic Activity in Cultured Renal Epithelial Cells—To determine the effects of hypertonicity on general endocytotic activity, $mCCD_{cl1}$ and LLC-AQP2 cells were subjected to isotonic (300 mosmol/kg) or hypertonic (500 mosmol/kg) medium for various periods of time in the presence of the fluid phase marker FITC-dextran (Fig. 11*A*). FITC-dextran internalization increased over time in both cell lines subjected to isotonic (300 mosmol/kg) conditions and was already visible 3 min after its addition to medium of LLC-AQP2 cells and 12 min after its addition to the medium of $mCCD_{cl1}$ cells. Importantly, hypertonicity significantly ($p < 0.05$) reduced FITC-dextran internalization over the entire period of time tested. We tested whether increased AQP2 cell surface expression by hypertonicity is mediated by a generalized decrease of endocytotic activity by treating LLC-AQP2 cells with 10 μM methyl-β-cyclodextrin (mβCD; Sigma), a cholesterol-depleting agent that reduces the rate of internalization of many membrane-bound proteins and receptors without affecting their intracellular trafficking back to the cell surface (40) (Fig. 11*B*). A shift of cell surface wild-type AQP2 was increased in LLC-AQP2 cells treated 30 min with mβCD as compared with AQP2 cell surface expression of non-treated cells. LLC-AQP2 (S256D) cells displayed even greater levels of AQP2 expressed at the cell surface following mβCD treatment (Fig. 11*B*, compare *1* and *2*). In addition, as previously described (25), mβCD induced strong AQP2 cell surface expression in LLC-AQP2 (S256A) cells (Fig. 11*B*, compare *3* and *4*). The absence of the AQP2 S256A mutant at the cell surface of hypertonicity-challenged cells (Figs. 5, 6, and 8–10) may be explained by its deviated trafficking to the *trans*-Golgi region, reflecting the idea that only AQP2 phosphorylated at Ser^{256} accumulates at the cell surface under these conditions. On the other hand, contrary to mβCD treatment, hypertonicity did not enhance AQP2 cell surface expression in LLC-AQP2 (S256D) cells (Fig. 11*B* and Figs. 5, 6, and 8–10), indicating that its effect on reduced AQP2 endocytosis is not as great as that achieved by mβCD treatment.

Since accumulation of AQP2 at the cell surface could also result from an increase in AQP2 exocytosis, we investigated the effects of hypertonicity on AQP2 exocytosis by measuring ssYFP in the medium of LLC-ssYFP cells that express wild-type AQP2 (Fig. 11*C*). Our recent data show that ssYFP and AQP2 are co-localized in the same secretory vesicles and that the majority of newly synthesized ssYFP is secreted from the cell, does not accumulate in endocytic compartments (*i.e.* early and recycling endosomes and lysosomes), and is not readmitted into the cell via endocytotic uptake (32). Time course experiments revealed a time-dependent accumulation of ssYFP in the medium of cells subjected to isotonic (300 mosmol/kg) conditions. As expected, simultaneous stimulation of cells with 10 nM VP and 10 μM forskolin significantly increased YFP secretion. Hypertonicity, on the other hand, significantly decreased YFP extracellular accumulation throughout the entire period of time investigated, indicating that accumulation of AQP2 at the cell surface by hypertonicity does not result from an increase of AQP2 exocytosis.

DISCUSSION

A large body of work has focused on mechanisms that govern accumulation of AQP2 at the cell surface in response to VP (9, 11, 13). This is the first study to directly address the effects of hypertonicity on AQP2 trafficking during the first minutes of hypertonic stimulation. A summary of our findings is schematically depicted in Fig. 12. Enhanced tissue water permeability by hypertonicity immediately following hypertonic challenge in the absence of VP was already described in 1964 in toad bladder (41). This was found to be associated with the appearance of luminal membrane aggregates (42) that are believed to represent clusters of water channels. Using two different renal cell lines and kidney slice preparations, we find that hypertonicity significantly alters AQP2 trafficking by inducing its accumulation in the proximity of the cell surface to levels comparable with that achieved by VP and by inducing its accumulation in a perinuclear region that corresponds to the *trans*-Golgi network. Our findings indicate that under hypertonic conditions, AQP2 constitutively recycles between the cell surface and the *trans*-Golgi network. Subsequent AQP2 cell surface expression requires its phosphorylation at Ser^{256}, whereas the nonphosphorylated form accumulates in the *trans*-Golgi region. Hypertonicity-induced accumulation of AQP2 at the cell surface occurred independently of a rise of cAMP concentration but did depend on p38, ERK1/2, and JNK MAPK activity. Finally, a decrease of AQP2 endocytosis, but not an increase of AQP2 exocytosis, may partly explain the effect of hypertonicity on AQP2 cell surface expression.

What is the physiological relevance of acute hypertonicity on AQP2 trafficking? Chronic exposure of cells to a hypertonic environment, a feature of the inner medullary interstitium, leads to increased levels of AQP2 abundance and insertion of AQP2 into the basolateral membrane (15, 20). These observations may reflect a physiological need to enhance transcellular water flux under extreme conditions of hypertonicity. Our results indicate that AQP2 at least partly accumulates at the cell

FIGURE 10. **AQP2 accumulation at the cell surface, but not the *trans*-Golgi region, following acute hypertonicity depends on JNK MAPK activity.** $mCCDc_{l1}$, LLC-AQP2, LLC-AQP2 (S256D), and LLC-AQP2 (S256A) cells were preincubated or not for 30 min with the JNK inhibitor SP600125 (*SP600*) and then challenged or not (*Ctl*) for 30 min with either NaCl-enriched hypertonic (500 mosmol/kg) medium or VP. Cells were fixed and stained with anti-c-*myc* (for $LLC\text{-}PK_1$ cells) or anti-AQP2 (for $mCCDcl_1$ cells) for analysis of AQP2 expression at the cell surface and *trans*-Golgi region. Representative immunofluorescent images of $mCCDc_{l1}$ (*A*), LLC-AQP2 (S256A) (*B*; *1* and *3*), and LLC-AQP2 (S256D) cells (*B*; *2* and *4*) depicting the effects of SP600125 on AQP2 trafficking under hypertonic conditions are shown. *Bar*, 7 μm (*A*) and 10 μm (*B*). *C*, AQP2 cell surface expression was determined as described under "Experimental Procedures." Results are mean ± S.E. ($n = 4$). **, $p < 0.01$.

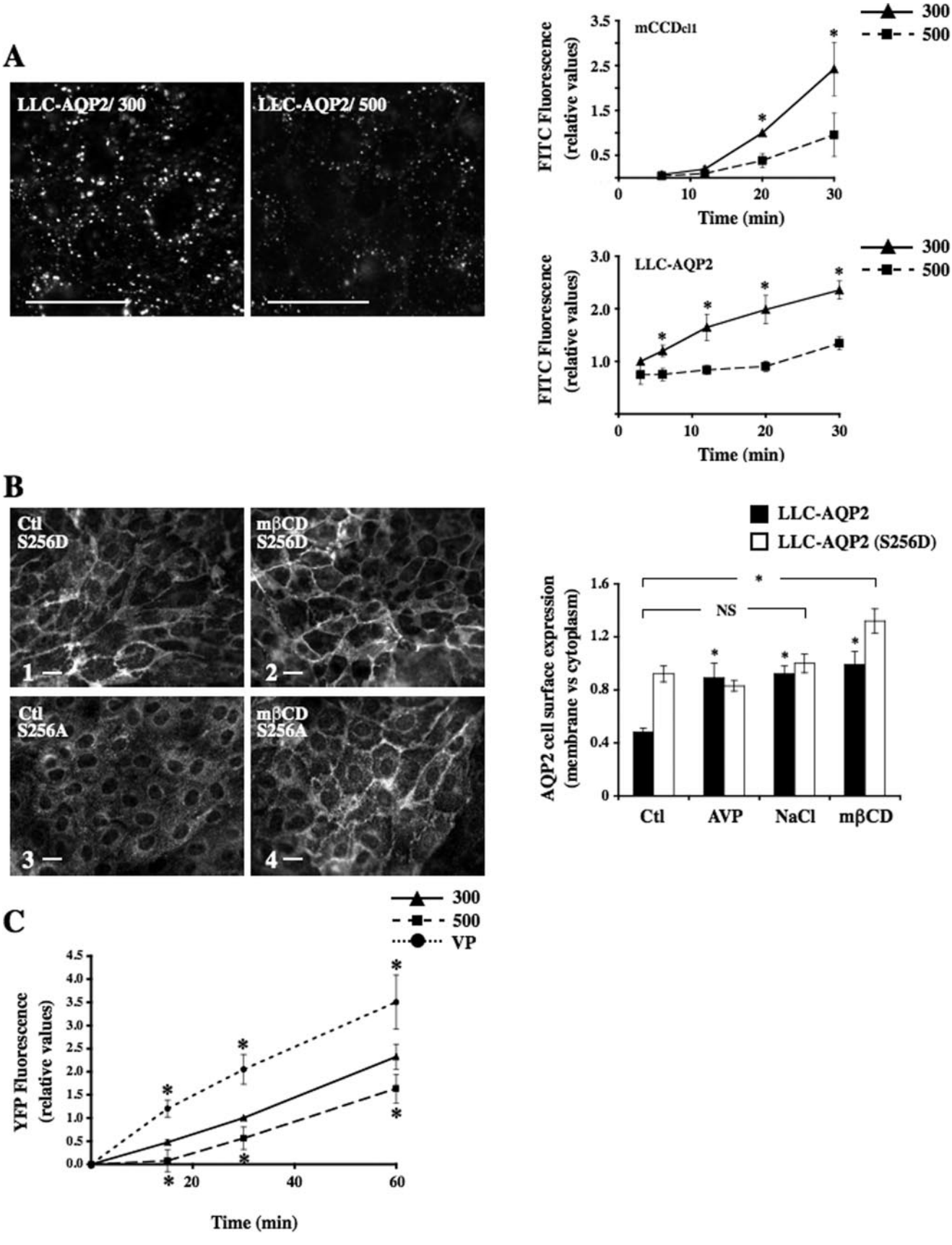
A
LLC-AQP2/ 300
LLC-AQP2/ 500
mCCDcl1
300
500
FITC Fluorescence (relative values)
Time (min)
LLC-AQP2
300
500
FITC Fluorescence (relative values)
Time (min)
B
Ctl S256D
mβCD S256D
Ctl S256A
mβCD S256A
1
2
3
4
LLC-AQP2
LLC-AQP2 (S256D)
AQP2 cell surface expression (membrane vs cytoplasm)
NS
Ctl
AVP
NaCl
mβCD
C
300
500
VP
YFP Fluorescence (relative values)
Time (min)

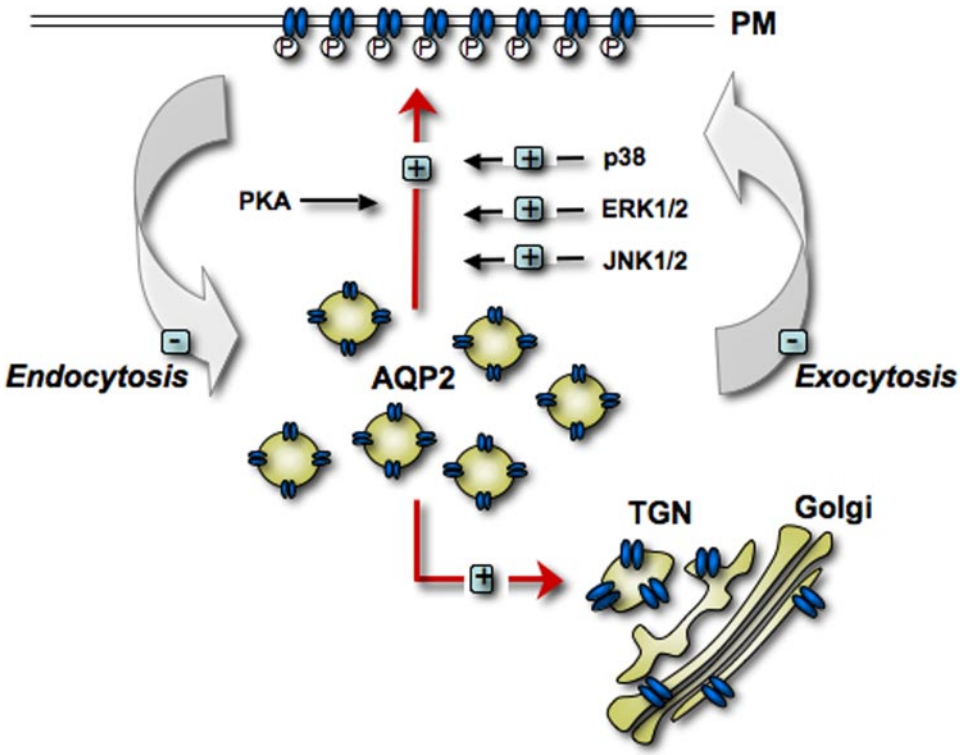

FIGURE 12. **Effects of acute hypertonicity on AQP2 trafficking.** Although AQP2 constitutively recycles between the cell surface and the TGN under hypertonic conditions, AQP2 accumulates at both of these regions at the onset of hypertonic challenge. Hypertonicity reduces both endocytotic and exocytotic activity in epithelial renal cells. Although AQP2 accumulation at the plasma membrane (*PM*) depends on both PKA activity and Ser^{256} phosphorylation, it occurs independently of a rise of intracellular cAMP. AQP2 accumulation at the plasma membrane, but not at the TGN, depends on an increase of hypertonicity-induced p38, ERK1/2, and JNK1/2 MAPK activity. Events that are induced by hypertonicity are depicted as a *plus sign*, and those that are repressed by hypertonicity are depicted as a *minus sign*.

apical surface at the onset of hypertoncity. Increased expression of AQP2 at the apical membrane immediately following hypertonic challenge may represent a first step to enhance transcellular water flux. Alternatively, apical membrane insertion of AQP2 in response to acute hypertonicity may play a role in the adaptation process triggered by hypertonic stress by helping to reduce intracellular water loss. Increased water efflux out of the cell via the basolateral membrane following an increase of interstitial osmolality may be partially counterbalanced by compensatory water entry from the nephron lumen via the apical membrane. The progressive decrease of apical AQP2 expression over longer periods of time could reflect the attainment of a balanced cell volume.

Hypertonicity induces activation of a network of protein kinases in a variety of cell types (5). Similar to results of the present study, p38, ERK1/2, and JNK MAPK activation by hypertonicity has been demonstrated in inner medullary collecting duct cells and in cells of the medullary thick ascending limb of Henle's loop (43–45). A role of p38, ERK and JNK in the transcriptional regulation of various aquaporins by hypertonicity has been shown in renal and lung epithelial cells and in astrocytes (45–47). Data from our present study indicate that MAPKs additionally participate in the accumulation of AQP2 at the plasma membrane, but not at the TGN, in renal CD principal cells immediately following hypertonic challenge. MAPK signaling has been shown to modulate intracellular trafficking of a number of receptors and transporters (48–53). Similar to observations of the present study, previous reports using inner medullary collecting duct cells indicate that urea induces activation of ERK1/2 (54, 55) but not p38 (55) and only induces weak activation of JNK as compared with the effect produced by NaCl and mannitol (43). Since urea did not induce accumulation of AQP2 at the cell surface, increased ERK1/2 activity alone by hypertonicity cannot account for increased AQP2 plasma membrane expression. The observed specificity of the pharmacological inhibitors used against p38, ERK1/2, and JNK MAPKs additionally indicates that increased AQP2 plasma membrane expression by hypertonicity requires activation of all three MAPKs, since reduced activity of a single kinase blocked the effect produced by hypertonicity. Several conclusions can be drawn from observations made in the present study on modulated AQP2 cell surface expression by p38, ERK, and JNK MAPKs. 1) The role that these MAPKs play in AQP2 plasma membrane expression is specific for hypertonic stimulation. 2) The effect of hypertonicity mediated by MAPKs occurs independently of an increase of cAMP concentration. 3) Activation of all three MAPKs is required for the hypertonicity-induced increase of AQP2 cell surface expression. 4) ERK1/2 and JNK may mediate AQP2 phosphorylation and/or dephos-

FIGURE 11. **Acute hypertonicity decreases both AQP2 endocytosis and exocytosis.** *A*, $mCCDc_{11}$ and LLC-AQP2 cells were challenged with isotonic (300 mosmol/kg) or hypertonic (500 mosmol/kg) medium in the presence of FITC-dextran for various periods of time (3–30 min) and were then rinsed and fixed. Representative immunofluorescent images of internalized FITC-dextran in LLC-AQP2 cells are shown after 20 min of exposure to either medium. *Bar*, 10 μm. FITC-dextran internalization was quantified as described under "Experimental Procedures" and expressed as the ratio of pixel intensity measured for each experimental condition and that measured in cells subjected to isotonic medium for 20 min (for $mCCDc_{11}$ cells) or 3 min (for LLC-AQP2 cells). Results are mean ± S.E. ($n = 4$). *, $p < 0.05$. *B*, LLC-AQP2 (S256D) (*1* and *2*), LLC-AQP2 (S256A) (*3* and *4*) and LLC-AQP2 cells (quantified as graphically depicted on the *right*) were maintained in isotonic medium and then exposed or not (control) to mβCD for 30 min prior to fixation and staining with an anti-c-*myc* antibody. *Bar*, 10 μm. AQP2 cell surface expression was determined as described under "Experimental Procedures." Results are mean ± S.E. ($n = 3$). *, $p < 0.05$. *NS*, not significant. *C*, LLC-ssYFP cells that express AQP2 and soluble secreted YFP were incubated in Hanks' buffer for 1 h and then stimulated or not (*300*) for 0–60 min with either NaCl-enriched hypertonic (500 mosmol/kg) medium or VP prior to collection of extracellular medium and analysis of YFP fluorescence. The ratio of YFP secretion, reflecting AQP2 exocytosis, is shown *between* each experimental condition, and cells were subjected to isotonic solution for 30 min in the absence of VP. Results are mean ± S.E. ($n = 5$). *, $p < 0.05$.

phorylation at Ser^{256}, since inhibition of ERK1/2 and JNK activity did not affect AQP2 cell surface expression in LLC-AQP2 (S256D) cells and did not affect VP-inducible cell surface expression of wild-type AQP2. 5) The role that p38 plays is distinct from than that of ERK1/2 and JNK, since inhibition of p38 activity led to a partial internalization of AQP2 in LLC-AQP2 (S256D) cells but did not affect the VP-inducible cell surface expression of wild-type AQP2. This indicates that p38 modulates the steady-state expression of AQP2 at the cell surface.

MAPKs may affect one or several events that govern AQP2 expression at the cell surface. Possibly, MAPKs, at least ERK1/2 and JNK, may mediate the phosphorylation process of AQP2 at Ser^{256} under hypertonic conditions. Since the PKA consensus sequence (RRQS^{256} in AQP2) is not an MAPK target, MAPK activation could enhance PKA-mediated phosphorylation of AQP2. Alternatively, modulated activity of proteins involved in AQP2 shuttling (11, 13, 56), such as SNAP, SNARE, and endocytotic adaptors, may be targeted by hypertonicity-induced signaling pathways. Finally, cytoskeleton remodeling plays a major role in AQP2 trafficking (13), and modulation of the cytoskeleton by hypertonicity may represent another means by which AQP2 cell surface accumulation is achieved.

Hypertonicity has previously been shown to activate the catalytic subunit of PKA (PKAc) in cultured renal CD cells (15). This occurs in the absence of an increase of cAMP concentration (this study). Increased AQP2 cell surface expression by hypertonicity nevertheless depends on PKA-dependent AQP2 phosphorylation at Ser^{256}, since hypertonicity did not induce expression of AQP2 at the surface of LLC-AQP2 (S256A) cells. Furthermore, it did not rescue the reduced cell surface expression of wild-type AQP2 in cells whose PKA activity was attenuated either by the PKA inhibitor PKI or following calmodulin-sensitive adenylyl cyclase type 3 inhibition, which reduces intracellular cAMP. Previous observations showed decreased AQP2 phosphorylation in response to hypotonicity (21), indicating that extracellular tonicity modulates the phosphorylation state of AQP2 at Ser^{256}. The observation that reduced AQP2 cell surface expression in LLC-AQP2 (S256D) cells treated with adenylyl cyclase type 3 inhibitors could be partially restored by hypertonicity, but not VP stimulation, suggests that in addition to AQP2 Ser^{256} phosphorylation, other PKA-mediated phosphorylation events are required for AQP2 cell surface accumulation. Previous observations suggest the occurrence of cAMP-PKA-dependent events that affect AQP2 trafficking independently of AQP2 Ser^{256} phosphorylation (12). In that study, dopamine or prostaglandin E_2 stimulation was found to induce AQP2 S256D endocytosis, but only in the presence of forskolin. Interestingly, AQP2 that accumulated in the *trans*-Golgi region immediately following hypertonic challenge was predominantly nonphosphorylated at Ser^{256}, as shown by AQP2 perinuclear accumulation in LLC-AQP2 (S256A) but not LLC-AQP2 (S256D) cells and by perinuclear accumulation of wild-type AQP2 in hypertonicity-challenged cells treated with calmodulin or PKA inhibitors. In addition to Ser^{256}, AQP2 phosphorylation at other sites (Ser^{261}, Ser^{264}, and Ser^{269}) has been shown to be regulated by VP (57–60). The influence of hypertonicity on the phosphorylation levels of these sites and ensuing consequences remain to be investigated.

Morphological studies have detected AQP2 in distinct intracellular pools, including early and recycling endosomes, TGN, and exocytic vesicles (34, 61). AQP2 was previously shown to constitutively recycle between recycling vesicles and the *trans*-Golgi region both under base-line conditions and following VP stimulation (34). In that study, at least part of the AQP2 pool residing in the *trans*-Golgi region was found to consist of internalized AQP2 initially expressed at the cell surface (34). In the present study, bafilomycin treatment abolished hypertonicity-induced AQP2 accumulation at the cell surface, whereas hypertonicity-induced accumulation of AQP2 at the TGN was reduced by VP stimulation. Taken together with transient AQP2 cell surface expression observed in principal cells of kidney slices exposed to hypertonic medium, our observations indicate that AQP2 constitutively recycles between the cell surface and the *trans*-Golgi region under hypertonic conditions and that only AQP2 phosphorylated at Ser^{256} accumulates at the cell membrane immediately following hypertonic challenge. After longer periods of hypertonic exposure in the absence of VP, AQP2 presumably accumulates in the *trans*-Golgi region as a Ser^{256}-nonphosphorylated form.

Hypertonicity is known to effectively impair clathrin-mediated endocytosis (62). Similar to AQP2, hypertonicity has been shown to double the expression of GLUT4 (glucose transporter 4) within 30 min in the plasma membrane of muscle cells (63). This event was found to rely on both reduced GLUT4 endocytosis and increased GLUT4 exocytosis. In hippocampal synapses, hypertonicity induced high intensity stimulation of neurotransmitter release that was attributed to fast recycling and reuse of synaptic vesicles (64), whereas hypertonicity inhibited exocytosis in neutrophils (65). The data of the present study indicate that increased AQP2 expression at the surface of CD principal cells can be attributed to a decrease of AQP2 endocytosis but not to an increase of AQP2 exocytosis. AQP2 endocytotic blockade induced by hypertonicity, however, is weaker than that following mβCD treatment and may account for the rapid decrease of hypertonicity-induced AQP2 cell surface expression following NaCl "washout" (*i.e.* reintroduction of hypertonicity-stimulated cells back to an isotonic medium) and for the time-dependent decay of the effect of hypertonicity observed in kidney slices.

In conclusion, the results of the present study indicate that acute hypertonic challenge profoundly affects AQP2 trafficking by inducing its accumulation at the cell surface, an event that depends on MAPK activity, and at the TGN. This in turn may have important physiological consequences on regulated water reabsorption and/or survival of renal medullary cells subjected to extreme conditions of hypertonicity.

Acknowledgment—We thank Prof. Bernard Rossier (Department of Pharmacology and Toxicology, University of Lausanne, Lausanne, Switzerland) for providing the $mCCD_{cl1}$ cell line.

REFERENCES

1. Van Hoek, A., Huang, Y., and Fang, P. (2001) in *Protein Adaptations and Signal Transduction*, pp. 73–85, Elsevier Science B.V., Amsterdam

2. Di Ciano-Oliveira, C., Thirone, A. C., Szaszi, K., and Kapus, A. (2006) *Acta Physiol.* (*Oxford*) **187,** 257–272
3. Nasuhoglu, C., Feng, S., Mao, Y., Shammat, I., Yamamato, M., Earnest, S., Lemmon, M., and Hilgemann, D. W. (2002) *Am. J. Physiol.* **283,** C223–C234
4. Rehn, M., Weber, W. M., and Clauss, W. (1998) *Pflugers Arch.* **436,** 270–279
5. Sheikh-Hamad, D., and Gustin, M. C. (2004) *Am. J. Physiol.* **287,** F1102–F1110
6. Handler, J. S., and Kwon, H. M. (2001) *Nephron* **87,** 106–110
7. Nahm, O., Woo, S. K., Handler, J. S., and Kwon, H. M. (2002) *Am. J. Physiol.* **282,** C49–C58
8. Brown, D., and Nielsen, S. (2004) in *Brenner & Rector's The Kidney*, 7th Ed. (Brenner, B. M., ed) pp. 573–597, Saunders, Philadelphia
9. Knepper, M. A. (1997) *Am. J. Physiol.* **272,** F3–F12
10. Katsura, T., Gustafson, C. E., Ausiello, D. A., and Brown, D. (1997) *Am. J. Physiol.* **272,** F817–F822
11. Brown, D. (2003) *Am. J. Physiol.* **284,** F893–F901
12. Nejsum, L. N., Zelenina, M., Aperia, A., Frokiaer, J., and Nielsen, S. (2005) *Am. J. Physiol.* **288,** F930–F938
13. Valenti, G., Procino, G., Tamma, G., Carmosino, M., and Svelto, M. (2005) *Endocrinology* **146,** 5063–5070
14. Ecelbarger, C. A., Nielsen, S., Olson, B. R., Murase, T., Baker, E. A., Knepper, M. A., and Verbalis, J. G. (1997) *J. Clin. Invest.* **99,** 1852–1863
15. Hasler, U., Vinciguerra, M., Vandewalle, A., Martin, P.-Y., and Feraille, E. (2005) *J. Am. Soc. Nephrol.* **16,** 1571–1582
16. Marples, D., Christensen, B. M., Frokiaer, J., Knepper, M. A., and Nielsen, S. (1998) *Am. J. Physiol.* **275,** F400–F409
17. Preisser, L., Teillet, L., Aliotti, S., Gobin, R., Berthonaud, V., Chevalier, J., Corman, B., and Verbavatz, J. M. (2000) *Am. J. Physiol.* **279,** F144–F152
18. Storm, R., Klussmann, E., Geelhaar, A., Rosenthal, W., and Maric, K. (2003) *Am. J. Physiol.* **284,** F189–F198
19. Hasler, U., Jeon, U. S., Kim, J. A., Mordasini, D., Kwon, H. M., Feraille, E., and Martin, P. Y. (2006) *J. Am. Soc. Nephrol.* **17,** 1521–1531
20. van Balkom, B. W. M., van Raak, M., Breton, S., Pastor-Soler, N., Bouley, R., van der Sluijs, P., Brown, D., and Deen, P. M. T. (2003) *J. Biol. Chem.* **278,** 1101–1107
21. Tamma, G., Procino, G., Strafino, A., Bononi, E., Meyer, G., Paulmichl, M., Formoso, V., Svelto, M., and Valenti, G. (2007) *Endocrinology* **148,** 1118–1130
22. Gaeggeler, H. P., Gonzalez-Rodriguez, E., Jaeger, N. F., Loffing-Cueni, D., Norregaard, R., Loffing, J., Horisberger, J. D., and Rossier, B. C. (2005) *J. Am. Soc. Nephrol.* **16,** 878–891
23. Bouley, R., Breton, S., Sun, T., McLaughlin, M., Nsumu, N. N., Lin, H. Y., Ausiello, D. A., and Brown, D. (2000) *J. Clin. Invest.* **106,** 1115–1126
24. Katsura, T., Verbavatz, J. M., Farinas, J., Ma, T., Ausiello, D. A., Verkman, A. S., and Brown, D. (1995) *Proc. Natl. Acad. Sci. U. S. A.* **92,** 7212–7216
25. Lu, H., Sun, T. X., Bouley, R., Blackburn, K., McLaughlin, M., and Brown, D. (2004) *Am. J. Physiol.* **286,** F233–F243
26. Bouley, R., Hawthorn, G., Russo, L. M., Lin, H. Y., Ausiello, D. A., and Brown, D. (2006) *Biol. Cell* **98,** 215–232
27. Yi, X., Bouley, R., Lin, H. Y., Bechoua, S., Sun, T.-X., del Re, E., Shioda, T., Raychowdhury, M. K., Lu, H. A. J., Abou-Samra, A. B., Brown, D., and Ausiello, D. (2007) **292,** F1303–F1313
28. Lencer, W. I., Brown, D., Ausiello, D., and Verkman, A. S. (1990) *Am. J. Physiol.* **259,** C920–C932
29. Breton, S., and Brown, D. (1998) *J. Am. Soc. Nephrol.* **9,** 155–166
30. Evan, G. I., Lewis, G. K., Ramsay, G., and Bishop, J. M. (1985) *Mol. Biol. Cell* **5,** 3610–3616
31. Bouley, R., Pastor-Soler, N., Cohen, O., McLaughlin, M., Breton, S., and Brown, D. (2005) *Am. J. Physiol.* **288,** F1103–F1112
32. Nunes, P., and Brown, D. (2007) in *The 5th International Conference of Aquaporin*, Nara, Japan
33. Bouley, R., Sun, T. X., Chenard, M., McLaughlin, M., McKee, M., Lin, H. Y., Brown, D., and Ausiello, D. A. (2003) *Am. J. Physiol.* **285,** C750–C762
34. Gustafson, C. E., Katsura, T., McKee, M., Bouley, R., Casanova, J. E., and Brown, D. (2000) *Am. J. Physiol.* **278,** F317–F326
35. Griffiths, G., and Simons, K. (1986) *Science* **234,** 438–443
36. Pearce, B. M., and Robinson, M. S. (1990) *Annu. Rev. Cell Biol.* **6,** 151–171
37. Futter, C. E., Gibson, A., Allchin, E. H., Maxwell, S., Ruddock, L. J., Odorizzi, G., Domingo, D., Trowbridge, I. S., and Hopkins, C. R. (1998) *J. Cell Biol.* **141,** 611–623
38. Christensen, B. M., Zelenina, M., Aperia, A., and Nielsen, S. (2000) *Am. J. Physiol.* **278,** F29–F42
39. Hoffert, J. D., Chou, C. L., Fenton, R. A., and Knepper, M. A. (2005) *J. Biol. Chem.* **280,** 13624–13630
40. Subtil, A., Gaidarov, I., Kobylarz, K., Lampson, M. A., een, J. H., and McGraw, T. E. (1999) *Proc. Natl. Acad. Sci. U. S. A.* **96,** 6775–6780
41. Bentley, P. J. (1964) *Comp. Biochem. Physiol.* **12,** 233–239
42. Bourguet, J., Chevalier, J., and Hugon, J. S. (1976) *Biophys. J.* **16,** 627–639
43. Berl, T., Siriwardana, G., Ao, L., Butterfield, L. M., and Heasley, L. E. (1997) *Am. J. Physiol.* **272,** F305–F311
44. Roger, F., Martin, P. Y., Rousselot, M., Favre, H., and Feraille, E. (1999) *J. Biol. Chem.* **274,** 34103–34110
45. Umenishi, F., and Schrier, R. W. (2003) *J. Biol. Chem.* **278,** 15765–15770
46. Arima, H., Yamamoto, N., Sobue, K., Umenishi, F., Tada, T., Katsuya, H., and Asai, K. (2003) *J. Biol. Chem.* **278,** 44525–44534
47. Hoffert, J. D., Leitch, V., Agre, P., and King, L. S. (2000) *J. Biol. Chem.* **275,** 9070–9077
48. Gu, Y., and Stornetta, R. L. (2007) *Acta Pharmacol. Sin.* **28,** 928–936
49. Moron, J. A., Zakharova, I., Ferrer, J. V., Merrill, G. A., Hope, B., Lafer, E. M., Lin, Z. C., Wang, J. B., Javitch, J. A., Galli, A., and Shippenberg, T. S. (2003) *J. Neurosci.* **23,** 8480–8488
50. Redman, P. T., He, K., Hartnett, K. A., Jefferson, B. S., Hu, L. S., Rosenberg, P. A., Levitan, E. S., and Aizenman, E. (2007) *Proc. Natl. Acad. Sci. U. S. A.* **104,** 3568–3573
51. Samuvel, D. J., Jayanthi, L. D., Bhat, N. R., and Ramamoorthy, S. (2005) *J. Neurosci.* **25,** 29–41
52. Soundararajan, R., Zhang, T. T., Wang, J., Vandewalle, A., and Pearce, D. (2005) *J. Biol. Chem.* **280,** 39970–39981
53. Zhu, Y., Pak, D., Qin, Y., McCormack, S. G., Kim, M. J., Baumgart, J. P., Velamoor, V., Auberson, Y. P., Osten, P., van Aelst, L., Sheng, M., and Zhu, J. J. (2005) *Neuron* **46,** 905–916
54. Cohen, D. M. (1996) *Proc. Natl. Acad. Sci. U. S. A.* **93,** 11242–11247
55. Tian, W., Boss, G. R., and Cohen, D. M. (2000) *Am. J. Physiol.* **278,** C372–C380
56. Barile, M., Pisitkun, T., Yu, M. J., Chou, C. L., Verbalis, M. J., Shen, R. F., and Knepper, M. A. (2005) *Mol. Cell Proteomics* **4,** 1095–1106
57. Fenton, R. A., Moeller, H. B., Hoffert, J. D., Yu, M. J., Nielsen, S., and Knepper, M. A. (2008) *Proc. Natl. Acad. Sci. U. S. A.* **105,** 3134–3139
58. Hoffert, J. D., Nielsen, J., Yu, M. J., Pisitkun, T., Schleicher, S. M., Nielsen, S., and Knepper, M. A. (2007) *Am. J. Physiol.* **292,** F691–F700
59. Hoffert, J. D., Pisitkun, T., Wang, G., Shen, R. F., and Knepper, M. A. (2006) *Proc. Natl. Acad. Sci. U. S. A.* **103,** 7159–7164
60. Lu, H. A., Matsuzaki, T., Bouley, R., Hasler, U., Qin, Q., and Brown, D. (2008) *Am. J. Physiol.* **295,** F290–F294
61. Tajika, Y., Matsuzaki, T., Suzuki, T., Aoki, T., Hagiwara, H., Kuwahara, M., Sasaki, S., and Takata, K. (2004) *Endocrinology* **145,** 4375–4383
62. Heuser, J. E., and Anderson, R. G. (1989) *J. Cell Biol.* **108,** 389–400
63. Li, D., Randhawa, V. K., Patel, N., Hayashi, M., and Klip, A. (2001) *J. Biol. Chem.* **276,** 22883–22891
64. Sara, Y., Mozhayeva, M. G., Liu, X., and Kavalali, E. T. (2002) *J. Neurosci.* **22,** 1608–1617
65. Rizoli, S. B., Rotstein, O. D., Parodo, J., Phillips, M. J., and Kapus, A. (2000) *Am. J. Physiol.* **279,** C619–C633